PB90 216474/AS

INVESTIGATION ON THE CAUSE OF NUMEROUS UPPER FLOOR FAILURES DURING THE 1985 MEXICO CITY EARTHQUAKE

by

Roberto Villaverde

A Technical Report of Research
supported by the
National Science Foundation
under
Grant No. BCS-8610871

Department of Civil Engineering
University of California, Irvine

November, 1989

APPENDIX VII

NATIONAL SCIENCE FOUNDATION
Washington, D.C. 20550

FINAL PROJECT REPORT
NSF FORM 98A

PLEASE READ INSTRUCTIONS ON REVERSE BEFORE COMPLETING

PART I—PROJECT IDENTIFICATION INFORMATION

1. Institution and Address
University of California, Irvine
Department of Civil Engineering
Irvine, CA 92717

2. NSF Program
EHM

3. NSF Award Number
BCS-8610871

4. Award Period
From 7/1/86 To 11/30/89

5. Cumulative Award Amount
$90 017

6. Project Title
Investigation on the Cause of Numerous Upper Floor Failures During the 1985 Mexico City Earthquake

PART II—SUMMARY OF COMPLETED PROJECT *(FOR PUBLIC USE)*

Presented herein are the results of a study carried out to investigate the prevalent factors that contributed to the collapse of the upper floors of a large number of buildings during the earthquake of September 19, 1985, in Mexico City. The study involves the review of the collected data regarding such collapses, an examination of the apparent causes of the phenomenon, the design of a typical 10-story frame structure according to the 1976 Mexico City building code, and the nonlinear analysis of one of its frames under one of the ground acceleration records from the earthquake. It is found that in many cases the upper floor collapses might have occurred because the large accelerations and long duration of the earthquake induced in the failed buildings the formation of plastic hinges at the columns of some of their upper stories and because these plastic hinges in turn induced the lateral instability of such stories and the ones above them. It is also found that in some frame structures this failure mechanism may result from (1) the degradation of the stiffness of their beams, (2) the consequent e-longation of their natural periods, (3) their response in a second or third mode and in resonance with the ground motion that excites them, and (4) their vibration in a mode not considered to be the predominant one in their design.

PART III—TECHNICAL INFORMATION *(FOR PROGRAM MANAGEMENT USES)*

1 ITEM *(Check appropriate blocks)*	NONE	ATTACHED	PREVIOUSLY FURNISHED	TO BE FURNISHED SEPARATELY TO PROGRAM: Check (✓)	Approx. Date
a. Abstracts of Theses	✓				
b. Publication Citations	✓				
c. Data on Scientific Collaborators	✓				
d. Information on Inventions	✓				
e. Technical Description of Project and Results		✓			
f. Other *(specify)*					

2. Principal Investigator/Project Director Name *(Typed)*	3. Principal Investigator/Project Director Signature	4. Date
Roberto Villaverde	Roberto Villaverde	11/1/89

NSF Form 98A (1-87) Supersedes All Previous Editions

Form Approved OMB No. 3145-0058

DEDICATION

This work is dedicated to the the victims of the earthquakes of September of 1985, for whom knowledge of earthquakes did not advance fast enough.

ACKNOWLEDGMENTS

The author wishes to express his sincere gratitude to the National Science Foundation, which, under Grant No. ECE-8610871, generously funded this investigation. Special thanks are extended to Dr. Manuel Portillo of the University of Chihuahua, Mexico, who suggested some of the ideas explored in this study. The contribution of Messrs. Samuel Young and Wei Chen, both graduate students at the University of California, Irvine, and the insightful adviced offered by Mr. Alberto Gutierrez, an engineer with many years of experience in structural design, on the common practice in the design of buildings in Mexico City are herein greatfully acknowledged. Deep appreciation is also due to Professor Roberto Meli of Instituto de Ingenieria, UNAM, who unselfishly allowed the author to go through the Instituto's records and photographs of the earthquake damage.

Any opinions, findings, and conclusions or recommendations expressed in this publication are those of the author and do not necessarily reflect the views of the National Science foundation.

TABLE OF CONTENTS

LIST OF TABLES

Table | Page

Page

LIST OF FIGURES

Page

Page

Page

Page

CHAPTER 1

INTRODUCTION

1.1 Background

The morning of September 19, 1985, Mexico City was struck by a strong earthquake ($M_S = 8.1$) that caused the loss of thousands of human lives and extensive damage to a large number of buildings. A damage survey (Meli et al., 1985; Rosenblueth and Meli, 1986) estimated the collapse of or severe damage to 330 multistory buildings, most of them with a reinforced concrete structure, between 3 and 13 stories high, and in sites, within an area of the city that was founded on an old lake bed, underlain by deposits of soft clay.

During the reconnaissance of the damage induced by the earthquake, a type of failure that stood out because of its recurrence and peculiarity was the collapse of the top stories of buildings (see as examples Figures 2.1 through 2.25). According to Meli et al. (1985), upper floor collapses were observed in 79 of the 210 cases (38 per cent) of collapse recorded. Of significance too was the fact that 62 per cent of the buildings with upper floor failures were built after 1957 (Meli and Miranda, 1986), which is an indication that a large number of them were designed and detailed according to modern building codes which require a comprehensive seismic design. Interestingly enough, such a large number of upper floor failures has not been observed during previous earthquakes in Mexico City (Meli and Miranda, 1986).

Many reasons have been given to explain the occurrence of so many upper floor collapses. Among the prevailing ones are: (a) the common practice in Mexico City of changing the cross section of columns with height; (b) inadequate reinforcement development lengths and splices; (c) excessive live loads in upper floors, which often were used for storage; (d) a whiplash effect induced by the interaction between soil and structure; (e) abrupt changes in the lateral stiffness of structural systems; (f) pounding between neighboring buildings; (g) the contribution of higher modes of vibration in structures designed for a distribution of lateral forces based on their fundamental mode; and (h) lack of seismic design. However, some of these factors can not satisfactorily explain why in such cases the damage concentrated in the upper stories and not in the lower ones or uniformly along the total building height. Similarly, contradictory arguments arise when one considers buildings with similar properties and under similar conditions which did not suffer any damage, not to say the collapse of their upper stories. Even further, most of them can not explain why the columns of such buildings failed (see

Figures 2.21 and 2.22) despite the fact that the implicit intention of building codes is to avoid the formation of plastic hinges in columns whenever the forces for which buildings are designed are exceeded. Thus, although undoubtedly the listed factors might have contributed to the upper floor failures in some cases, those without an apparent cause of failure and the large number of buildings that experienced this type of collapse seem to indicate that the criteria used in the design of these buildings somehow failed to insure the integrity of their columns and, hence, seem to suggest the existence of a possible weakness in such design criteria.

1.2 Related Work

Although upper floor failures have been observed in previous earthquakes, in Mexico City as well as in other cities around the world, the September 1985 earthquake has been perhaps the first to cause such a large number of them. Thus, no direct attention has been given to this problem before. Nonetheless, it is of interest to note that some studies have found some evidence of weaknesses in seismic code procedures, and that these weaknesses may affect primarily the upper floors of a building. For example, Portillo and Ang (1976) report that in two 10-story reinforced concrete frame structures designed according to the 1974 SEAOC code, the probabilities of yielding for the columns of the buildings' upper stories are higher than they are for the columns of the lower ones, and higher than the corresponding probabilities for their respective connecting beams. They conclude, thus, that the equivalent lateral force procedure recommended by the 1974 SEAOC code may lead to building designs with weak columns and strong beams at their upper stories. They also observe that in comparison with a dynamic analysis, calculations based only on the fundamental mode of a structure may underestimate the probablities of yielding of its upper floors. Along the same lines, Chopra and Cruz (1986), in an evaluation of the equivalent lateral force procedures recommended by ATC-3, the 1976 Mexico City code, and the Uniform Building Code, conclude that the formulas in these procedures do not properly recognize the participation of modes of vibration higher than the fundamental one, particularly for structures with high fundamental periods. Similarly, Neuss, Maison, and Bouwkamp (1983), in studying five multistory buildings with steel frame structures and ranging in height from 15 to 60 stories, evaluate the significance of their higher modes of vibration in their peak seismic response. They find that although overall their fundamental modes are the dominant ones in all cases, the contribution of the higher modes is increasingly important towards the top of the buildings. In one case, for example, the higher modes contribute about 50 per cent to the total story shear at the roof of the building. Of special significance are the findings of Clough, Benuska and Wilson (1965), who analyzed a stiff (fundamental natural period = 1.60 sec.) and a flexible (fundamental natural period = 2.77 sec.) 20-story frame building under the N-S component of the 1940 El

Centro earthquake and noticed that in both structures the columns of the top four floors yielded while the lower ones remained in their elastic range. Finally, it is pertinent to note too that Corly (1986), in his survey of the damage in Mexico City after the 1985 earthquake, observed numerous cases in which plastic hinges formed in columns instead of in beams.

1.3 Object and Scope

In view of the lack of a satisfactory explanation for the observed upper floor failures and the need to identify possible deficiencies in the current earthquake-resistant design practice, a formal investigation was carried out to find out what were indeed the prevalent factors that contributed to the occurrence of the phenomenon. The investigation involved the collection and review of the available data from the recorded cases of upper floor collapses, an examination of the apparent causes of the collapses, the identification of common characteristics among the buildings that experienced such type of failure, and the search for inadequacies in the Mexico City building code recommendations for the design of buildings with such characteristics. In an effort to uncover unknown failure mechanisms, the study included too the design of one of the frames of a typical 10-story reinforced concrete frame structure in accordance to the 1976 Mexico City building code and the common design practice in this city, and the simulation of its response under the 1985 earthquake by means of a nonlinear analysis under one of the ground acceleration records from the earthquake.

1.4 Organization

This report is divided into five chapters. The collected data on the buildings that suffered the collapse of their upper floors during the 1985 earthquake are summarized in Chapter 2. Presented also in this chapter are some of the statistics obtained from these data and some of the conclusions drawn from the analysis of the data and such statistics.

The simulation study of the designed 10-story structure is described in Chapter 3, where the details of the design of the structure are also given. As a means to validate the model and procedures used in the simulation study, Chapter 3 includes too a comparison between the calculated response of a structure in Mexico City that experienced the effects of the 1985 earthquake and the damage that it reportedly suffered.

On the basis of results from the simulation study, an analysis is then made of the possible causes of the upper floor collapses in Mexico City and, based on this analysis, an explanation is offered for the occurrence of such upper floor collapses. Such an analysis and such an explanation are presented in Chapter 4.

Finally, the main findings of the study and recommendations for further research are summarized in Chapter 5.

CHAPTER 2

DAMAGE DATA

2.1 Collected Data

Relevant literature and the data gathered by the Instituto de Ingeniería of UNAM on the damage caused by the 1985 earthquake was reviewed and, on the basis of these data, the buildings listed in Table 2.1 were identified as cases for which the damage consisted only of the collapse of one or more of their upper stories. In total, seventy four buildings were found to have suffered upper floor collapses, although it should be noted that Meli and Miranda (1986) report a total of seventy nine cases. Table 2.1 gives the location of these buildings as well as the type of occupancy, the original number of stories, an approximate date of construction, the type of structure, estimated geometry in plan, the number of collapsed stories, and the reported apparent cause of failure, whenever one was more or less evident from the visual inspection of the damage.

The photographs in Figures 2.1 through 2.25 illustrate the upper floor collapses of some of the buildings listed in Table 2.1.

2.2 Statistics of Upper Floor Collapses

In reviewing the data discussed above, it was found, first of all, that all the buildings with upper floor collapses were located on the area of the city which is underlain by deposits of soft, highly compressible clay. Then, it was found that upper floor failures were experienced by buildings with 4 to 15 stories. It is noted, however, that the largest number corresponded to buildings with 8 (15 cases), 7 (14 cases), 5 (13 cases), and 9 (11 cases) stories. As far as the year of construction is concerned, it was learned that the largest number of buildings with upper floor collapses corresponded to those built between 1957 and 1976; that is, the time interval between the first building code with comprehensive recommendations for seismic design and the significantly revised version that was implemented afterwards. Concerning the type of structure, it was observed that upper floors collapses were equally predominant in buildings with frame and waffle-slab structures [interestingly enough, Meli and Miranda (1986) report that 52% of the failures in structures with flat plates were in upper floors], and that only a few had a structural system based on load-bearing brick walls. Furthermore, it is worthwhile to note that while almost all the failed buildings had reinforced concrete structures, three buildings with steel structures also experienced the collapse of their upper floors. In like manner, it was noticed that the geometry of their floor plan was rectangular for most buildings, although there were some cases with a triangular or an irregular floor plan. It was noted too that only a few had variations in their plan area along their height. Finally, in regard to the apparent cause of failure, it was observed that in some cases there was a clear evidence of pounding between adjacent buildings; important torsional effects, particularly in the case of corner buildings; overloaded floors, as in the case of some garment factories and government buildings; and a lack of seismic design, as it was true for those constructed in the 1940s. Notwithstanding, it was found that many of the buildings with upper floor collapses did not show an evidence of the cause that might have contributed to the collapse of their upper floors, except, of course, the failure of their columns (see Figures 2.21 and 2.22, for example).

2.3 Conclusions from Damage Data

On the basis of the damage data reviewed, it was learned that the upper floor collapses were not a phenomenon affecting only one type of structural system, one construction material, or a certain plan configuration. It was learned too that the phenomenon was most frequent in frame structures with 5 to 9 stories, and that it is reasonable to expect that these buildings shared a common, albeit unknown, characteristic that made them vulnerable to this type of collapse. Furthermore, it was concluded that a lack of seismic design, pounding, overloading, a sudden change of stiffness from one floor to another, and unaccounted torsional motions could not explain all the upper floor collapses observed and, hence, that these could not have been the only factors that led to such upper floor collapses.

CHAPTER 3

SIMULATION STUDY

3.1 Purpose

Although the analysis of the data from the observed cases of buildings with upper story collapses allows one to draw some conclusions about the phenomenon, it fails nonetheless to give a general and satisfactory explanation for its occurrence. Therefore, to gain a further insight into the problem, it was decided to design a reinforced concrete frame structure according to the recommendations of the 1976 Mexico City building code [10] as well as the design procedures followed by most design offices in this city, and simulate its response to the 1985 earthquake by means of a time-history analysis under one of the ground acceleration records from the earthquake.

3.2 Selected Model

Since it was obvious that the phenomenon of upper floor collapses involved inelastic deformations, it was considered necessary to perform the time-history analysis taking into account the post-elastic behavior of beams and columns. The program Drain-2D (Kannan and Powell, 1975) was thus selected for the analysis, modeling the columns of the structure as beam-column elements and its beams as reinforced-concrete beam elements with stiffness degradation. Damping was assumed proportional to the mass matrix of the structure and equal to five per cent of critical in its fundamental mode. P-delta effects and shear deformations were neglected. In addition, the structure was considered to be fixed at its base; that is, soil-structure interaction was neglected. However, the joint regions between beams and columns were assumed perfectly rigid to account for the fact that plastic hinges form near the faces of a joint region rather than at the theoretical center lines of beams and columns. The live load considered was the live load specified by the code for the seismic design of the structure. Although it is recognized that the value of live load specified by the code represents an upper bound, the use of this value in the simulation study was considered appropriate given that during the inspection of the damage by the 1985 earthquake many buildings were found to be overloaded. Besides, after experimenting with different values of live load, it was determined that live load did not represent a significant parameter in a building's nonlinear response.

The beam-column element in the program assumes a bilinear moment-rotation relationship at the ends of the element and takes into account the interaction between axial force and bending moment to determine when the element yields. Yielding is assumed to occur when combined an axial force and a bending moment define a point that lies outside a simplified axial force-bending moment interaction diagram. In defining thus the moment-rotation relationships for the beam-elements used in the analysis, a strain hardening modulus of two per cent of the initial modulus of elasticity was, arbitrarily, selected. Similarly, in defining their axial force-bending moment interaction diagrams, the formulas given in the 1976 Mexico City building code [11] for the ultimate pure axial load, the ultimate pure bending moment, and the axial load and bending moment for the balanced condition of compression members were considered. Their moments of inertia were assumed to be equal to 1.5 times the values calculated with Eq. 10-10 in Reference 1 (considering no sustained load), which is a flexural rigidity formula recommended by the 1983 ACI code to determine the effective length of long reinforced concrete columns. The factor of 1.5 was introduced to account for the fact that in comparison with the results from experimental tests the formula represents a lower bound. Thus, by multiplying this lower bound by 1.5, an average value rather than a lower bound one is obtained [see Figure 10.11.5 (a) in Reference 2].

As with the beam-column element, the reinforced concrete beam element assumes a bilinear moment-rotation relationship at the end of the element, but in this case this moment-rotation relationship also considers a degrading flexural stiffness. The hysteretic model used is an extended version of Takeda model, although the latter can also be selected as an option. In addition, this element neglects axial deformations and, hence, yielding takes place only under the effect of a bending moment. Thus, for the beam elements in the simulation study the Takeda model with a strain hardening stiffness equal to two percent of the initial one was selected. Their moments of inertia were calculated using the formulas recommended by the 1983 ACI code (Eq. 9-7 in Reference 1 and Eq. 1 in Section 9.5.2.4 of Reference 2) to determine the short-term deflections of continuous beams. The moments of inertia so calculated give an intermediate value between the values obtained assuming an uncracked cross section and a fully cracked. As a reinforced concrete beam is never uncracked nor fully cracked along its entire length, it is believed that these values give a realistic representation of the actual flexural rigidity of a reinforced concrete beam which has some of its cross sections stressed at levels near their yield limits. The yield moment for the beam elements was defined as the ultimate moment for doubly reinforced T beams. As in the case of beam-columns, the formulas of the 1976 Mexico City building code [11] were used to calculate such ultimate moments.

Note that as the application of Drain-2D is limited to two-dimensional structures, the simulation study was necessarily restricted to structures whose behavior is essentially two-dimensional.

3.3 Earthquake Excitation

The excitation selected for the analysis was the worst-case combination of the two horizontal ground acceleration records obtained at the Secretaria de Comunicaciones y Transportes (SCT) station (Mena et al., 1985). This worst-case combination was obtained by adding vectorially the two available components from this station and selecting the combination with the largest peak ground acceleration. It was found, thus, that the component along the S60E direction represented such a worst case and that in such direction the peak ground acceleration was 0.188 g. The ground acceleration time-history for this component and the corresponding acceleration response spectrum for 0, 2, 10 and 20 per cent damping are depicted in Figures 3.1 and 3.2, respectively.

As the SCT station is located on the soft soil area of Mexico City, and since all upper floor collapses occurred in this soft soil area, it is believed that the selected excitation is, if not a close approximation, at least representative of the ground motion experienced by the buildings that suffered such type of collapse. This in spite of the obvious differences owing to the different depths of the soft soil deposits at different locations.

3.4 Model Verification

In order to assess the effectiveness of the model adopted and the selected excitation in predicting the damage induced by the 1985 earthquake, one of the interior longitudinal frames of an existing building in Mexico City whose damage during this earthquake has been reported in the literature (Meli and López, 1986; Avila and Meli, 1987) was analyzed first. The building is an office building [administrative offices of Sistema de Transporte Colectivo (STC)] with 10 stories and a basement, located in the old lakebed area of the city, and built around 1971. Its foundation is of the box type with a depth of 3 meters, partially compensated, and supported by 87 friction piles, each 22 meters in length. Its structure is of reinforced concrete with rectangular floors, frames in the longitudinal (E-W) direction, and coupled shear walls in the transversal (N-S) one (see Figures 3.3 through 3.5). The nominal 28-day strength of the concrete considered in its design was of 240 kg/cm^2, while the nominal yield strength of the steel reinforcement was of 4000 kg/cm^2. The modulus of elasticity of the concrete was assumed to be 1500000 $T\text{-}m^2$ in all cases. The gravitational loads considered are those recommended for an office building in Reference 12 and given for this particular building in Table 3.1. The cross sections of the beams and columns of the analyzed frame, together with their respective steel reinforcements, are depicted in Figures 3.6 and 3.7. The effective moments of inertia of its beams and columns and their ultimate axial loads and ultimate bending moments are summarized in Tables 3.2 and 3.3, respectively. The first six natural periods of the frame, calculated on the basis of effective moments of inertia and rigid joints, are listed in Table 3.4.

Note that a particular advantage of the configuration of this building is the minimal biaxial action of its longitudinal frames, as most of the lateral forces in the transversal direction are taken by the shear walls. It is adequate, thus, to model this type of structure as a two-dimensional one. It is pertinent to mention too that this building was designed for the increased seismic loads recommended for critical facilities, that at the joints where a verification was made the columns had a flexural yield strength which was greater than that of the corresponding concurrent beams, that the shear reinforcement in its columns was plentiful and with good detailing, and that in general the quality of its construction was above average (Avila and Meli, 1987).

The frame described above was thus subjected to the first 70 seconds of the excitation selected for the analysis, after which the location of the plastic hinges formed in the frame was recorded. The analysis was carried out for only 70 seconds out of the total 180 seconds which comprise the total length of the record in order to reduce computer costs (a trial analysis using the actual duration of the record took 3 hours of CPU time in a VAX/VMS 785). However, this time interval covers the strongest part of the excitation and the time at which the frame reaches its maximum displacements. It is believed, thus, that no additional plastic hinges are formed after the 70 seconds used in the analysis.

Figure 3.8 shows the plastic hinges which according to the computer analysis would have formed in the structure if it had been subjected to a ground motion identical to the SCT record. This distribution of plastic hinges may be thus contrasted with the actual damage the structure suffered during the 1985 earthquake, damage that is shown schematically in Figure 3.9. Note that except for the plastic hinges at the lower ends of the columns of the first floor, which do not appear in the description of the actual damage, the pattern of damage seems to be adequately predicted by the computer model. Furthermore, one notices that such plastic hinges do show in one of the exterior rectangular frames of the building (see Figure 3.10), a fact that suggests that perhaps the plastic hinges at the bottom of the interior frame were there but somehow were overlooked during the damage survey.

In conclusion, if one takes into account the unavoidable uncertainties in the characteristics of the ground motion at the exact site of the building, the possible soil-structure interaction effects neglected by the model, and the limitations of the computer program itself (e.g., bilinear yield interaction diagrams as opposed to the actual curvilinear ones), the above comparison shows that the model can predict the damage pattern reasonably well and that the selected analytical model can therefore be used with some confidence.

3.5 Building Design

Once confirmed the satisfactory accuracy of the computer model adopted, a reinforced concrete building structure assumed located in the soft soil area of Mexico City was designed following strictly the 1976 building code for this city [10]. The selected building was an office building with the same number of stories, same structural configuration, same floor plan, same dimensions, and same material properties as those for the STC building described in the previous section (see Figures 3.3 through 3.5). However, different cross sections were considered to study the effect of the reduction of beam and column sizes with height, which is something that is commonly practiced in Mexico City, and to study a structure for which most of its beams and columns are not overdesigned to satisfy minimum reinforcement requirements. Such a building structure was thought to be appropriate for this investigation because its configuration is typical of medium high-rise buildings in Mexico City, because its height is representative of those that suffered upper floor collapses during the 1985 earthquake, and because the regularity of its geometry allows an easy interpretation of its behavior. In addition, it was flexible enough to have a fundamental natural period close to the dominant period of the ground motion recorded at SCT during that earthquake, and, thus, large incursions into its nonlinear range of behavior were likely.

The design of the building was based on the static method

[10] and the simplifications that are commonly made in Mexico City's design offices (e.g., gross moments of inertia, a fixed foundation, and center-to-center spans). The static method is recommended by the code for structures with a height of less than 60 meters and assumes, when no reductions are considered, a triangular distribution of lateral forces with height. In applying this method, the gravitational loads described in Table 3.1, a seismic coefficient of 0.24 divided by a ductility factor of 4, and an accidental eccentricity for the center of mass of each level equal to 3.6 m in the longitudinal direction and to 1.8 m in the transverse one were used. The analysis of the building was carried out using the computer program Super-Etabs [15,25]. From this analysis, the natural periods and story drifts listed respectively in Tables 3.5 and 3.6 were obtained. The natural periods in Table 3.5, which correspond to the first six, were computed considering the three-dimensional character of the building, the simplifications mentioned above, and the final choice for the cross sections of its beams and columns. The story drifts contained in Table 3.6 are those for the longitudinal direction of the building and were determined by multiplying by the ductility factor of four considered in the analysis the values obtained under the design seismic loads. These story drifts were considered to be adequate despite the fact that some slightly exceeded the limit of 0.008 specified by the code to avoid damage to nonstructural elements attached to the structure. The internal forces in the beams and columns of the building were calculated

using the following load factors and load combinations:

(a) 1.4 DL + 1.4 LL

(c) 1.1 DL + 1.1 LLL + 0.33 LEL + 1.1 TEL

where

DL = dead load

LL = live load for vertical load analysis

LLL = live load for lateral load analysis

LEL = earthquake load along longitudinal direction

TEL = earthquake load along transverse direction

Finally, selecting the internal forces corresponding to the critical load combination in each case, the beams and columns of the interior longitudinal frames of the building were proportioned following the recommendations for the design of reinforced concrete structures given in Reference 11. The cross sections and steel reinforcements obtained are shown in Figures 3.11 and 3.12.

3.6 Time-History Analysis of Designed Building

The next step toward the purpose stated in Section 3.1 was to study the behavior of the designed building under the 1985 earthquake. To this end, one of its interior longitudinal frames was analyzed under the first 70 seconds of the earthquake excitation described in Section 3.3 using the computer program

Drain-2D and the model introduced in Section 3.2. The moments of inertia and the ultimate loads and moments of the beams and columns of the frame, needed for the analysis and calculated as indicated in Section 3.2, are summarized in Tables 3.7 and 3.8. Its first six natural periods when rigid joints and effective moments of inertia are considered are given in Table 3.9.

The results of the analysis are presented in Figures 3.13 through 3.20. These figures show how the formation of plastic hinges at the beams and columns of the frame progresses throughout the duration of the excitation. It can be seen from them that under the S60E component of the SCT ground acceleration record the frame remains elastic (i.e., no plastic hinges) for about the first 24 seconds and that after that time plastic hinges form at the lower ends of the columns of the first floor and at the ends of a large number of the lower beams of the frame. Subsequently, the formation of plastic hinges propagates upwardly to other beams and, eventually, at about 64 seconds after the beginning of the excitation, plastic hinges develop at the upper ends of all the columns of the 8th and 9th stories. Thus, owing to the formation of plastic hinges at these columns, it is clear that after this time the frame would develop a failure mechanism in which, first, the columns of the 9th story undergo large lateral displacements, then these columns fail by instability, and ultimately the 9th and 10th stories collapse (see Figure 3.21).

3.7 Redesign of 10-story building

Although the analysis presented in the previous section clearly showed that it was possible to have in a frame structure a type of failure which involves only the collapse of its upper floors, it was felt necessary to investigate if such a failure could occur only in structures with rather flexible upper stories, as it was the case for the analyzed one. In an effort to try to answer this question, the building described in Section 3.5 was thus redesigned considering stiffer elements for the upper part of the structure. With this idea in mind, the cross sections of beams and columns were changed to match those of the original STC building referred to in Section 3.4. That is, the cross sections of the exterior columns as well as those of all the beams were kept constant along the height of the building. Corresponding to these cross sections are the natural periods and longitudinal story drifts given in Tables 3.10 and 3.11. Note that the fundamental natural period of the building is now only slightly shorter than in the previous case , but the story drifts of the upper stories are considerably smaller.

The dimensions of the new cross sections for the beams and columns of the interior frames of the building as well as the steel reinforcement required for these new cross sections are shown in Figures 3.22 and 3.23.

3.8 Time-history Analysis of Redesigned Building

Once established the characteristics of the new structural elements of the building, the nonlinear time-history analysis described in Section 3.6 was repeated, as before, for one of its interior longitudinal frames using the new loads and new properties corresponding to such new structural elements. The moments of inertia and ultimate loads and moments required to perform this analysis were calculated as previously described, obtaining the values listed in Tables 3.12 and 3.13. The procedure to carry it out was also the same, except that in this case the lengths of the beams and columns of the frame were assumed equal to those measured between the axes of these elements. The reason behind this exception was simply that by doing so one obtains a more flexible structure than when one considers rigid joints, and that it may thus, given that joints are not perfectly rigid nor totally flexible, represent a more critical case. The first six natural periods for this frame under the assumption of center-to-center lengths and effective moments of inertia are given in Table 3.14.

Figure 3.24 summarizes the results of the analysis. This figure shows where plastic hinges are formed after the analyzed frame is subjected to 70 seconds of the exciting ground motion. It can be seen that although plastic hinges were formed at some of the columns of the sixth and eighth stories, in this case the frame did not develop enough plastic hinges to form a collapsing mechanism. Hence, it was concluded that under the considered excitation this building would not experience the collapse of its upper floors.

Based on the results presented above, it was logical at first to accept the fact that indeed the stiffer building was not susceptible to an upper floor collapse, and hence that the upper floor failure mechanism observed in the previous case could be explained on the basis of the flexibility of its upper stories. On second thoughts, however, it was realized that a possible reason the redesigned frame did not develop enough plastic hinges to form a failure mechanism could have been that the considered excitation did not induced, because of the dynamic characterists of this particular structure, a sufficiently strong response. To verify, then, this idea, the analysis was repeated with a magnified ground motion obtained by multiplying the accelerations of the SCT, S60E, record by a factor of 1.5. The results, presented as for the first design in a way that shows how plastic hinges develop with time, are depicted in Figures 3.25 through 3.29. As expected, it can be seen from these figures that in this case too the structure was eventually led to the collapse of its upper stories.

CHAPTER 4

EXPLANATION FOR UPPER FLOOR COLLAPSES

4.1 Introductory Remarks

The simulation study presented in the preceding chapter demonstrates that reinforced concrete frame structures designed with the 1976 Mexico City building code may indeed be susceptible to the collapse of their upper floors. It does not give, however, a clue about what causes or leads to this kind of failure. In this chapter, therefore, an attempt is made to understand why such type of failure can happen in spite of the fact that by specifying larger safety factors for columns than it does for beams the code implicitly intends to avoid plastic deformations in columns and hence floor collapses.

4.2 Influence of Higher Modes of Vibration

As mentioned in Section 1.2, several studies have pointed out that since the static method for the seismic design of buildings basically assumes a first-mode response, it sometimes does not properly recognize the participation of higher modes of vibration in the upper part of a structure. Therefore, the first step in the search for a logical explanation of the phenomenon of upper floor collapses was an evaluation of the degree of approximation involved in the use of this method. For this purpose, the maximum interstory shears induced by the SCT, S60E, ground motion on the interior longitudinal frame analyzed in Section 3.6 were calculated, by means of a dynamic analysis and under the assumption of a perfectly elastic structure, considering first only the response in its first mode and then the response in all of its modes. The comparison between the two sets of values obtained is presented in Figure 4.1, from which it can be seen that the higher modes of this structure did not contribute significantly to its total response to the ground motion used in the analysis. Furthermore, from this comparison one may conclude that the distribution of the actual lateral forces on the frame, when subjected to above ground motion and before it reached its first yielding, could not have been significantly different from the distribution of the lateral forces for which the frame was designed. Accordingly, it was concluded too that the plastic hinges which appeared in the columns of the eighth and ninth stories of the frame during the nonlinear time-history analysis carried out in Section 3.6 could not have been induced by not taking into account higher-mode responses in the design of the frame.

4.3 Distribution of Shear Forces Before Failure

In view of the fact that the aforementioned upper column plastic hinges could not be explained on the basis of the participation of the frame's higher modes, it was decided to investigate how the shear forces were distributed along its height just before such plastic hinges were formed. The outcome of this investigation is summarized in Figure 4.2, where are given the instantaneous magnitudes and directions of such forces 58.35 seconds after the beginning of the excitation.

Figure 4.2 unambiguously shows that at the time of 58.35 seconds, which is about six seconds before the first plastic hinges in the upper columns of the frame were detected in the analysis reported in Section 3.6, the structure was vibrating in a mode that resembles the third mode shape of a shear beam. Thus, to further investigate this finding, the natural periods of the frame were calculated for the case when, as indicated in Figure 4.3, the lower ends of the columns of its first story are hinged and the flexural stiffnesses of its beams from the first to the eight floors are neglected. The obtained first three such natural periods are listed in Table 4.1.

The fact that the distribution of lateral forces seconds before the plastic hinges in the upper columns of the frame were formed corresponded to a distribution that is typical of a third mode, and the fact that at that instant the third natural period of the structure was close to 2 sec., i.e., the dominant period of the SCT record (see response spectrum in Figure 3.2), clearly suggested that around that time the structure was vibrating predominantly in its third mode and in resonance with the ground motion. This in turn suggested that perhaps the cause of the formation of such plastic hinges was that the structure was designed to vibrate primarily in its first mode, but that in actuality it was vibrating, some time after incurring into its post-elastic range, in its third mode. Thus, to confirm this idea, a comparison was made between the interstory shears for which the frame under investigation was designed and those induced by the SCT ground motion when it is assumed that that the frame vibrates purely in its third mode, that the natural period of its third mode is 2 seconds, and that the corresponding damping ratio is 5 per cent. The comparison is depicted in Figure 4.4, from which it can be observed that if the structure indeed vibrates under the conditions stated above, it will exceed its design shears only at its top two stories.

4.4 Failure Mechanism

The analysis presented above offers what it seems to be a reasonable explanation for the observed behavior of the analyzed frame in the simulation study of Section 3.6 and hence for the phenomenon of upper floor collapses. This explanation can be enunciated as follows:

Because of the large intensity of the ground motion, plastic hinges formed at the bottom of the columns of the first story and at most of the beams of the structure. This behavior was in accordance with the design criteria, which presume inelastic action of the beams if the design forces are exceeded. But because of the development of plastic hinges and the deterioration of the beams, the natural periods of the structure were e-longated in such a way that the structure was forced to vibrate in its mode with the natural period that was the closest to the predominant period of the ground motion: its third mode. This, together with the large ground accelerations which the structure was still subjected to after it entered into its inelastic range and the fact that its columns were designed for a first-mode distribution of shear forces, induced the formation of plastic hinges in the columns of some of its upper stories and the consequent lateral instability of these stories.

CHAPTER 5

CONCLUSIONS

5.1 Summary

Data from the numerous cases of upper floor collapses observed during the earthquake of September 19, 1985, in Mexico City were presented and scrutinized, and on the basis of these data factors apparently responsible for such collapses were examined. Additionally, in an effort to understand the phenomenon behind such collapses, a study was carried out to simulate the response to that earthquake of a typical 10-story frame structure designed according to the 1976 Mexico City Building Code and the common design practice in this city.

5.2 Conclusions

On the basis of the reviewed data and the results from the performed simulation study, the following conclusions are drawn:

1. The upper floor collapses observed during the earthquake of September 19, 1985, were a phenomenon that affected buildings with different number of stories, different structural systems, different construction materials, diverse geometric character-

istics, and designed according to different versions of the local building code.

2. A lack of seismic design, pounding, overloading, a sudden change of stiffness from one floor to another, unaccounted torsional motions, and the influence of higher modes of vibration can not explain all the upper floor collapses observed and hence they could not have been the only factors that led to such collapses.

3. It is possible to have in a reinforced concrete frame structure a failure mechanism generated by the formation of plastic hinges in the columns of some of its upper stories capable of inducing the lateral instability of these stories. The plastic hinges in columns may, in turn, be induced by story shears which, because of changes in the dynamic properties of the structure after it experiences inelastic deformations, exceed those for which the structure was designed.

4. Under a given ground motion, a structure can experience the collapse of its upper floors if:

   (a) the second or third natural period of the structure is shorter than the dominant period of the ground motion, and

   (b) the ground motion is characterized by strong accelerations before and after the structure incurs into its inelastic range of behavior.

The first condition is necessary to assure that the second or third natural period of the structure can enlongate to a value close to the dominant period of the ground motion after the structure suffers some deterioration and, hence, that after this deterioration its predominant mode of vibration can be its second or third mode. The second condition is necessary so that the structure can, first of all, go into its inelastic range and suffer the aforementioned deterioration, and, secondly, its members can be subjected afterwards to internal forces that exceed the internal forces for which they were designed.

5.3 Recommendations for Future Research

The findings listed above imply, first of all, that the phenomenon of upper floor collapses can also occur in other parts of the world and, secondly, that present building provisions, which allow inelastic deformations but do not require an inelastic analysis, may not be sufficient to avoid this type of phenomenon. Therefore, additional studies are needed to investigate if the same type of phenomenon can occur in the seismic regions of the United States in buildings designed with U.S. codes under earthquake ground motions with the characteristics of those that have been recorded in the U.S. Further research is also needed to identify for which geometric and structural characteristics and under which class of ground motions a building could be susceptible to the collapse of its upper stories. In this regard, it is important that the three-dimensional character of structures be considered to investigate the influence of torsional motions in the occurrence of the phenomenon. Finally, new design criteria and changes to current code recommendations should be developed and their effectiveness in preventing upper floor collapses validated.

REFERENCES

1. American Concrete Institute, Building code requirements for reinforced concrete (ACI 318M-83), Detroit, Michigan, June 1984.

2. American Concrete Institute, Commentary on building code requirements for reinforced concrete (ACI 318M-83), Detroit, Michigan, June 1984.

3. J. Avila and R. Meli, Análisis de la respuesta de edificios típicos ante el sismo del 19 de septiembre de 1985, Report to Conacyt, Instituto de Ingeniería, UNAM, July 1987.

4. J. Avila and R. Meli, "Análisis de la respuesta de un edificio típico ante el sismo del 19 de septiembre de 1985," VII Congreso Nacional de Ingeniería Sísmica, Querétaro, Qro., November 19-21, 1987, pp. D162-176.

5. A.K. Chopra and E.F. Cruz, "Evaluation of building code formulas for earthquake forces," Journal of Structural Engineering, ASCE, Vol. 112, No.8, August 1986.

6. R.W. Clough, K.L. Benuska, and E.L. Wilson, "Inelastic earthquake response analysis of tall buildings," Proceedings of the Third World Conference on Earthquake Engineering, Auckland and Wellington, New Zealand, 1965, pp. 2.68-89.

7. G. Corley, "Consequences of the September 19, 1985 in Mexico City," Concrete International: Design & Construction, Vol. 8, No. 1, January 1986.

8. J. Damy Rios, "Impresiones del día 19 de septiembre de 1985," Revista IMCYC, No. 176, Vol. 23, December-January 1986, pp.85-94.

9. R. Hanson, "Performance of steel structures," Proceedings of the International Conference on The Mexico Earthquakes-1985: Factors Involved and Lessons Learned, Mexico City, September 19-21, 1986, pp.350-363.

10. Instituto de Ingeniería, Universidad Nacional Autónoma de México, Manual de diseño por sismo según el reglamento de construcciones para el Distrito Federal, Publication No. 406, Mexico City, Mexico, July 1977

11. Instituto de Ingeniería, Universidad Nacional Autónoma de México, Diseño y construcción de estructuras de concreto: normas técnicas complementarias del reglamento de construcciones para el Distrito Federal, Publication No. 401, Mexico City, Mexico, July 1977.

12. Instituto de Ingeniería, Universidad Nacional Autónoma de México, Requisitos de seguridad y servicio para las estructuras, Publication No. 400, Mexico City, Mexico, July 1977.

13. International Masonry Institute, Mexico earthquake September, 1985, Earthquake Investigation Report, October 1986.

14. A. E. Kannan and G. H. Powell, Drain-2D, A general computer program for dynamic analysis of inelastic plane structures, Report No. EERC 73-22, University of California, Berkeley, August 1975.

15. B.F. Maison and C.F. Neuss, Super-Etabs: An enhanced version of the Etabs program, Report to the National Science Foundation, J.G Bouwkamp, Inc., January 1983.

16. R. Meli et al., Efectos de los sismos de septiembre de 1985 en las construcciones de la Ciudad de Mexico: Aspectos estructurales, Segundo Informe del Instituto de Ingeniería de la Universidad Nacional Autónoma de México, Instituto de Ingeniería, UNAM, November, 1985.

17. R. Meli and C. López, Evaluación de los efectos de los sismos de septiembre de 1985: Parte II, Evaluación detallada de edificios típicos, Report No. DE/EST, Vol. 2-1, Instituto de Ingeniería, UNAM, October 1986.

18. R. Meli and E. Miranda, "Aspectos estadísticos de los daños ocasionados por los sismos de septiembre de 1985," V Congreso Nacional de Ingeniería Sísmica, Veracruz, Ver., April 30-May 3, 1986, pp. (A4)01-11.

19. R. Meli, E. Miranda and N. Riqaud, Evaluación de los efectos del los sismos de septiembre de 1985 en los edificios de la Ciudad de México: Parte I, Evaluación de daños, Report No. DE/EST, Vol. 2-1, Instituto de Ingeniería, UNAM, October 1986

20. E. Mena et al., Acelerograma en el Centro SCOP de la Secretaría de Comunicaciones y Transportes: Sismo del 19 de septiembre de 1985, Informe IPS-10B, Instituto de Ingeniería, UNAM, September 1985.

21. D. Mitchell, "Structural damage due to the 1985 Mexican earthquake," 5th Canadian Conference on Earthquake Engineering, Ottawa, July 6-8, 1987, pp. 87-111.

22. C.F. Neuss, B.F. Maison, and J.G. Bouwkamp, A study of computer modeling formulations and special analytical procedures for earthquake response of multistory buildings, Report to National Science Foundation, J.G. Bouwkamp, Inc., January 1983.

23. M. Portillo-Gallo and A. H-S Ang, Evaluation of safety of reinforced concrete buildings to earthquakes, Structural Research Series No. 439, University of Illinois, Urbana, Ill., October 1976.

24. E. Rosenblueth and R. Meli, "El sismo del 19 de septiembre de 1895: Sus efectos en la Ciudad de Mexico", Revista IMCYC, No. 180, Vol. 24, May 1986, pp. 15-31.

25. E.L. Wilson, J.P. Hollings and H.H Dovey, Etabs: Three dimensional analysis of building systems (extended version), Report No. UCB/EERC 75-13, Earthquake Engineering Research Center, University of California, Berkeley, California, March 1979.

Table 2.1. Buildings with upper floor collapses in Mexico City during the earthquake of September 19, 1985

No.	Location	Use	No. of stories	Date of construction	No. of collapsed stories	Type of structure	Geometry in plan	Apparent cause of failure
1	Hidalgo & Reforma	Office	5	1984	2	R.C. frames	Rectangular	Failure of columns
2	B. Dominguez # 64	Office	5	1950	3	R.C. frames	Rectangular	Overloading
3	Palma N. # 513	Office	8	1950's	6	R.C. frames	Rectangular	Pounding
4	Allende # 59	Factory	7	1950's	3	Unknown	Rectangular	Added floors
5	Cjon. San Camilito	Residential	8	1967	6	R.C. flat plates and brick walls	Rectangular	Failure slab-col. joints
6	2do. Cjon. Mixcalco # 46	Warehouse and factory	5	1950's	4	R.C. frames	Rectangular	Undeterminable
7	Alarcon # 1	Garment factory	5	1950's	3	R.C. flat plates	Rectangular	Overloading
8	A. Circunvalacion & J. Herrera	Office	5	1975	2	R.C. flat plates	Rectangular	Punching shear
9	Juarez # 117	Office	7	1940's	4	R.C. frames	Irregular	Pounding
10	Morelos # 98	Office	9	1950's	4	R.C. flat plates	Rectangular	Failure of cols.
11	Londres # 18	Residential	10	1970	2	R.C. flat plates	Rectangular	Pounding
12	Reforma & Roma	Hotel	11	1960	3	R.C. frames	Irregular	Failure of cols.
13	Madrid # 58	Office	8	1940's	6	R.C. flat plates	Irregular	Failure of cols.
14	Atenas & Lisboa	Office	7	1980's	5	R.C. frames	Rectangular	Excessive torsion
15	Hamburgo & Dinam.	Office	5	1965	3	R.C. frames	Rectangular	Excessive torsion

Table 2.1 (continued). Buildings with upper floor collapses in Mexico City during the earthquake of September 19, 1985

No.	Location	Use	No. of stories	Date of construction	No. of collapsed stories	Type of structure	Geometry in plan	Apparent cause of failure
16	Liverpool and Berlin	Residential	9	1955	5	R.C. flat plates and brick walls	Rectangular	Failure of cols.
17	Bucareli # 20	Cffice	8	1950's	3	R.C. frames	Rectangular	Pounding
18	Vallarta # 21 (centro)	Office	5	1960's	1	R C. frames and brick walls	Rectangular	Pounding
19	La Fragua # 4	Office	9	1950	4	R.C. frames	Rectangular	Pounding
20	Uruguay # 14	Parking	9	1970	5	R.C. flat plates	Rectangular	Pounding
21	Isabel la Catolica & V. Carnza.	Office	11	Unknown	6	R.C. floors ans steel frames	Rectangular	Undeterminable
22	Palma # 5	Retail	8	1950	4	R.C. flat plates	Rectangular	Ovldng. & pounding
23	20 de Nov. & Regina	Office & factories	8	1965	3	R.C. flat plates	Rectangular	Ovldng. & pounding
24	Chimalpopoca & F. S.T. Mier	Garment factory	12	1950's	6	R.C. flat plates	Rectangular	Overloading
25	J.M. Izazaga & I. catolica	Garment factory	6	1973	3	R.C. flat plates	Rectangular	Overloading
26	Regina # 15	Office & warehouse	7	1960's	5	R.C. flat plates	Rectangular	Excessive torsion
27	F.S.T. Mier nr. P. Suarez	Unknown	9	Unknown	2	Unknown	Rectangular	Vertical setbacks
28	F.S.T. Mier # 154	Factory	9	1970's	4	R.C. flat plates	Irregular	Excessive torsion
29	Nezahualcoyotol # 130	Factory and retail	8	1973	5	R.C. frames	Rectangular	Overloading

Table 2.1 (continued). Buildings with upper floor collapses in Mexico City during the earthquake of September 19, 1985

No.	Location	Use	No. of stories	Date of construction	No. of collapsed stories	Type of structure	Geometry in plan	Apparent cause of failure
30	J.M. Izazaga # 89	Office & retail	15	1973	4	R.C. flat plates	Irregular	Punching shear
31	Pino Suarez # 83	Factory & retail	9	1967	7	R.C. flat plates	Rectangular	Overloading
32	S. Antonio Abad no #	Unknown	8	Unknown	4	Unknown	Unknown	None
33	Independencia # 59	Office	10	1940's	6	R.C. frames	Rectangular	No seismic design
34	L. Cardenas & 16 de Sept.	Residential	5	1940's	2	R.C. floors and steel frames	Rectangular	Failure of cols.
35	L. Cardenas # 21	Office & retail	8	1940's	3	Steel braced frames	Rectangular	Undeterminable
36	Art. 123 & L. Moya	Office	4	1960's	1	R.C. frames	Rectangular	Undeterminable
37	Tonala # 190	Office	7	1960's	2	Brick shear walls	Triangular	None
38	Cordoba # 17	Office	7	1960's	Undetermined	Unknown	Rectangular	None
39	Tonala & A. Obregon	Office	4	1960's	3	R.C. flat plates	Rectangular	Vertical setbacks
40	Nuevo Leon # 66	Office	7	1960's	5	Unknown	Rectangular	Offset elevator walls
41	A. Obregon # 240	Residential	7	1960's	Undetermined	R.C. frames	Rectangular	None
42	Guanajuato # 119	Office	8	1960's	4	R.C. frames and brick walls	Rectangular	None
43	Monterrey and Guanajuato	Office	7	1960's	6	R.C. frames and brick walls	Rectangular	Failure of cols.
44	A. Obregon & Insurg.	Office	8	1960's	6	R.C. flat plates	Triangular	None

Table 2.1 (continued). Buildings with upper floor collapses in Mexico City during the earthquake of September 19, 1985

No.	Location	Use	No. of stories	Date of construction	No. of collapsed stories	Type of structure	Geometry in plan	Apparent cause of failure
45	Chapultepec # 334	Office	5	1960's	2	Flat plates with R.C. & brk. walls	Rectangular	Vertical setbacks
46	Yucatan & Insurg.	Office	7	1960's	1	R.C. flat plates	Irregular	None
47	Insurg. & Zacatecas	Unknown	7	Unknown	1	Unknown	Triangular	None
48	Tehuantepec # 12	Residential	11	1976	6	Unknown	Unknown	Vertical setbacks
49	Yucatan # 71	Residential	8	1974	6	R.C. flat plates & brk. walls	Rectangular	None
50	Chiapas # 129	Office	6	1976	Undeterminable	R.C. flat plates & brk walls	Irregular	None
51	Laredo & Tamaulipas	Unknown	8	Unknown	6	Unknown	Irregular	Excessive torsion
52	Rio de la Loza # 136	Unknown	9	Unknown	Undeterminable	Unknown	Unknown	None
53	F.S.T. Mier & D. 20 Nov.	Unknown	4	Unknown	1	R.C. frames	Unknown	None
54	Chimalpopoca & D. 20 Nov.	Unknown	5	1950's	2	Unknown	Unknown	None
55	Bouterini & Tlalpan	Unknown	7	1965	3	R.C. flat plates	Unknown	None
56	Cuauhtemoc & Chapultepec	Unknown	5	1965	2	R.C. flat plates & brk. walls	Unknown	None
57	Tlalpan & A. Taller	Unknown	8	Unknown	6	Unknown	Unknown	None
58	Cuauhtemoc acrs. # 36	Unknown	6	1962	3	Unknown	Unknown	None

Table 2.1 (continued). Buildings with upper floor collapses in Mexico City during the earthquake of September 19, 1985

No.	Location	Use	No. of stories	Date of construction	No. of collapsed stories	Type of structure	Geometry in plan	Apparent cause of failure
59	Dr. Velazco & Dr. Andrade	Unknown	6	Unknown	4	Unknown	Unknown	None
60	Dr. Vertiz & R. Lora	Office	8	Uknown	Unknown	Unknown	Unknown	None
61	Chiapas & Tonala	Office	5	Unknown	3	Unknown	Unknown	None
62	Univ. & Xola	Office	10	1950's	3	R.C. frames	Rectangular	None
63	Cuauhtemoc & Puebla	Unknown	6	Unknown	4	Unknown	Unknown	None
64	Insurg. & Guanajuato	Unknown	10	Unknown	3	R.C. frames	Irregular	None
65	Medellin & A. Obregon	Unknown	5	Unknown	3	Unknown	Unknown	None
66	Insurg. & Monterrey	Unknown	7	Unknown	3	Unknown	Unknown	None
67	Insurg. & Puebla	Unknown	9	Unknown	2	Unknown	Unknown	None
68	Tlalpan & J.M. Oton	Unknown	6	1960's	3	R.C. flat plates	Unknown	None
69	Dr. Velazco & Dr. Andrade	Unknown	4	1984	1	R.C. frames	Unknown	None
70	Dr. Liceaga # 12	Unknown	12	1970	2	R.C. flat plates	Unknown	None
71	F.S.T. Mier # 77	Unknown	14	1979	3	R.C. flat plates	Unknown	None
72	Tlalpan & G. Najera	Unknown	9	1965	3	R.C.frames & flt. plts.	Unknown	None
73	Cuauhtemoc & Colima	Office	9	1957	3	R.C. frames	Rectangular	None
74	L. Cardenas & Dr.	Unknown	7	1965	3	R.C. flat plates	Unknown	None

Table 3.1. Gravitational loads

Dead Load.- Typical floor	
10-cm concrete slab	240 Kg/m2
required additional slab weight	20
mortar	60
required additional mortar weight	20
floor finish	52
gypsum mortar	23
partitions and cladding	100
miscellaneous	25
Total	540 Kg/m2
Dead load.- Roof	
10-cm concrete slab	240 Kg/m2
required additional slab weight	20
tezontle fill	62
water proofing	30
gypsum mortar	23
miscellaneous	25
Total	400 kg/m2

Live load for vertical load analysis:

Typical floor: $120 + 420/\sqrt{A}$ (Kg/m2)

where A = tributary area

Roof: 100 Kg/m2

Live load for seismic analysis:

Typical floor: 90 Kg/m2

Rc[illegible] [illegible]0 Kg/m2

Table 3.2. Properties of beams of interior longitudinal frame of original SCT building

Floors	Moment of inertia (m4)		Positive ultimate moment (T-m)			Negative ultimate moment (T-m)		
	Beam A-B	Beam B-C	End A	End B	End C	End A	End B	End C
1-3	0.02472	0.02483	70.61	70.61	70.62	128.94	128.94	137.14
4-7	0.02416	0.02733	70.57	61.39	61.40	97.75	97.56	106.36
7-10	0.03725	0.03725	45.00	45.00	45.00	81.41	81.41	81.41

Note: properties of beams are symmetric about axis C

Table 3.3. Properties of columns of interior longitudinal frame of original SCT building

Stories	Column	Moment of inertia (m4)	Ultimate moment (T-m)	Ultimate load		Balanced	State
				Compression (T)	Tension (T)	Ultimate moment (T-m)	Ultimate load (T)
1-2	Exterior	0.01564	86.50	933.80	207.80	147.70	336.70
	Interior	0.02427	185.10	1176.90	461.30	234.90	337.80
3-4	Exterior	0.01564	86.50	933.80	207.80	147.70	336.70
	Interior	0.01797	127.70	1095.30	461.30	136.80	414.20
5-6	Exterior	0.01564	86.50	933.80	207.80	147.70	336.70
	Interior	0.00793	63.90	770.60	207.80	98.70	257.40
7-10	Exterior	0.01564	86.50	933.80	207.80	147.70	336.70
	Interior	0.00454	41.40	645.20	162.20	66.00	216.80

Table 3.4. First six natural periods of interior longitudinal frame of original SCT building considering rigid joints and effective moments of inertia

Mode	Natural period (sec)
1	1.627
2	0.554
3	0.314
4	0.215
5	0.162
6	0.128

Table 3.5. First six natural periods of designed 10-story building considering center-to-center lengths and gross moments of inertia

Mode	Natural period (sec)
1	1.682
2	1.000
3	0.684
4	0.647
5	0.379
6	0.263

Table 3.6. Story drifts in longitudinal direction of designed 10-story building under design seismic loads

Story	Story drift
10th	0.0040
9th	0.0072
8th	0.0080
7th	0.0092
6th	0.0084
5th	0.0092
4th	0.0084
3rd	0.0080
2nd	0.0080
1st	0.0064

Table 3.7. Properties of beams of interior longitudinal frame of designed 10-story building

Floors	Moment of inertia (m^4)		Positive ultimate moment (T-m)			Negative ultimate moment (T-m)		
	Beam A-B	**Beam B-C**	**End A**	**End B**	**End C**	**End A**	**End B**	**End C**
1-3	0.03151	0.03151	52.15	52.15	52.15	78.09	78.09	78.09
4-7	0.02549	0.02549	34.16	34.16	34.16	62.76	62.76	62.76
7-9	0.01742	0.01742	17.38	17.38	17.38	46.34	46.34	46.34
10	0.01330	0.01330	14.68	14.68	14.68	21.09	21.09	21.09

Note: properties of beams are symmetric about axis C

Table 3.8. Properties of columns of interior longitudinal frame of designed 10-story building

Stories	Column	Moment of inertia (m^4)	Ultimate moment (T-m)	Ultimate load		Balanced	State
				Compression (T)	Tension (T)	Ultimate moment (T-m)	Ultimate load (T)
1-2	Exterior	0.01309	49.70	851.10	121.70	113.70	336.80
	Interior	0.01309	49.70	851.10	121.70	113.70	336.80
3-4	Exterior	0.00953	39.70	752.50	103.90	92.40	295.00
	Interior	0.00953	39.70	752.50	103.90	92.40	295.00
5-6	Exterior	0.00669	25.50	649.00	81.10	73.20	252.90
	Interior	0.00669	25.50	649.00	81.10	73.20	252.90
7-8	Exterior	0.00447	21.70	567.40	81.10	56.10	213.80
	Interior	0.00447	21.70	567.40	81.10	56.10	213.80
9-10	Exterior	0.00279	18.00	485.80	81.10	40.90	174.60
	Interior	0.00279	18.00	485.00	81.10	40.90	174.60

Table 3.9. First six natural periods of interior longitudinal frame of designed 10-story building considering rigid joints and effective moments of inertia

Mode	Natural period (sec)
1	1.790
2	0.693
3	0.405
4	0.286
5	0.213
6	0.180

Table 3.10. First six natural periods of redesigned 10-story building considering center-to-center lengths and gross moments of inertia

Mode	Natural period (sec)
1	1.564
2	0.972
3	0.653
4	0.524
5	0.296
6	0.251

Table 3.11. Story drifts in longitudinal direction of redesigned 10-story building under design seismic loads

Story	Story drift
10th	0.0020
9th	0.0032
8th	0.0048
7th	0.0056
6th	0.0064
5th	0.0068
4th	0.0072
3rd	0.0076
2nd	0.0080
1st	0.0068

Table 3.12. Properties of beams of interior longitudinal frame of redesigned 10-story building

Floors	Moment of inertia (m^4)		Positive ultimate moment (T-m)			Negative ultimate moment (T-m)		
	Beam A-B	Beam B-C	End A	End B	End C	End A	End B	End C
1-3	0.02465	0.03501	68.53	68.53	52.15	94.24	94.24	78.09
4-7	0.03743	0.03807	42.18	42.18	42.12	77.90	77.90	65.52
7-10	0.03872	0.04141	42.12	42.12	41.93	65.52	65.52	39.59

Note: properties of beams are symmetric about axis C

Table 3.13. Properties of columns of interior longitudinal frame of redesigned 10-story building

Stories	Column	Moment of inertia (m^4)	Ultimate moment (T-m)	Ultimate load		Balanced	State
				Compression (T)	Tension (T)	Ultimate moment (T-m)	Ultimate load (T)
1-2	Exterior	0.01730	84.90	933.80	207.80	147.40	335.00
	Interior	0.01730	84.90	933.80	207.80	147.40	335.00
3-4	Exterior	0.01507	66.10	890.00	162.20	129.60	335.90
	Interior	0.01288	74.70	852.20	207.80	122.00	295.50
5-6	Exterior	0.01420	53.50	855.90	126.70	122.60	333.90
	Interior	0.00924	63.20	770.60	207.80	98.60	255.80
7-8	Exterior	0.01420	53.50	855.90	126.70	122.60	333.90
	Interior	0.00634	53.80	689.00	207.80	77.20	215.90
9-10	Exterior	0.01420	53.50	855.90	126.70	122.60	333.90
	Interior	0.00535	41.40	645.20	162.20	66.00	216.80

Table 3.14. First six natural periods of interior longitudinal frame of redesigned 10-story building considering center-to-center lengths and effective moments of inertia

Mode	Natural period (sec)
1	1.928
2	0.661
3	0.380
4	0.267
5	0.204
6	0.164

Table 4.1. First three natural periods of interior longitudinal frame of designed 10-story building when lower ends of first-story columns are hinged and stiffness of beams from first to eighth floors are neglected

Mode	Natural period (sec)
1	39.01
2	3.58
3	2.07

Figure 2.1. Building on Ave. Cuauhtemoc and Puebla

Figure 2.2. Building on Medellin and Ave. A. Obregón

Figure 2.3. Building on Puebla near Ave. de los Insurgentes

Figure 2.4. Building on Juárez No. 117

Figure 2.5. Building on Hamburgo and Dinamarca

Figure 2.6. Building under construction on Ave. Hidalgo and Paseo de la Reforma (Banco de México)

Figure 2.7. Building on Monterrey and Guanajuato (photograph after J. Damy Rios, 1986).

Figure 2.8. Building on I. La Catolica and V. Carranza (photograph after J. Damy Rios, 1986)

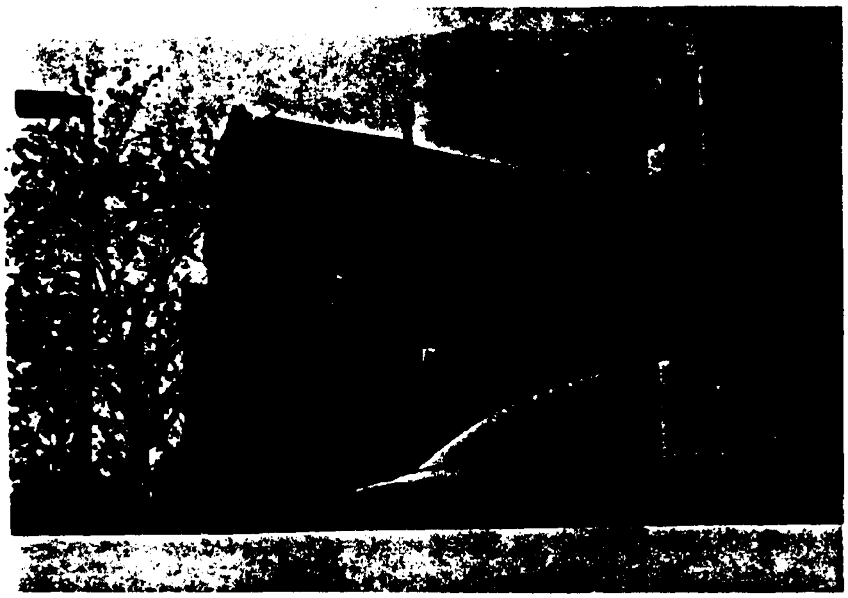

Figure 2.9. Building on San Antonio Abad (photograph after J. Damy Rios, 1986)

Figure 2.10. Building on Ave. de los Insurgentes and Monterrey

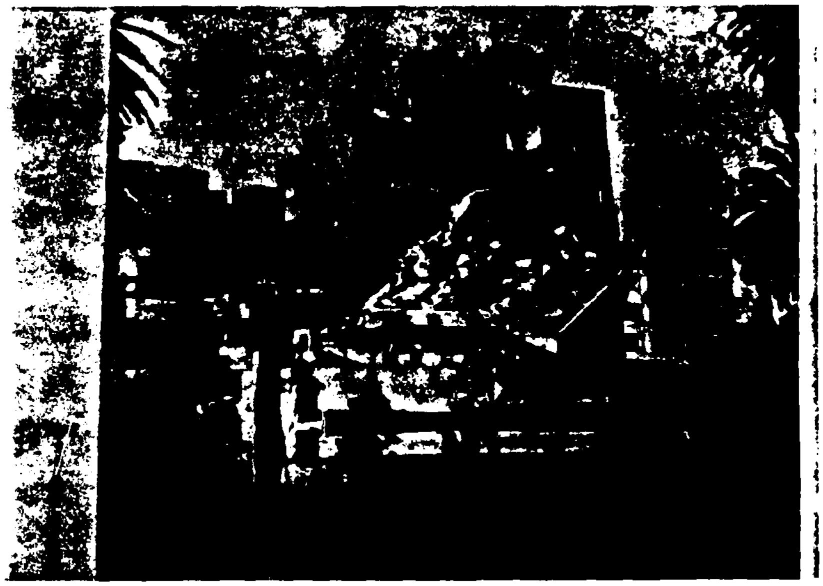

Figure 2.11. Building on Laredo and Tamaulipas (photograph after J. Damy Rios, 1986)

Figure 2.12. Building on Independencia No. [illegible], corner with Luis Moya (photograph after J. Damy Rios, 1986)

Figure 2.13. Building on Ave. Cuauhtemoc and Colima (Secretaria de Comercio y Fomento Industrial; photograph after J. Damy Rios, 1986)

Figure 2.14. Building on Ave. Universidad and Xola (Secretaria de Comunicaciones y Transportes; photograph after International Masonry Institute, 1986)

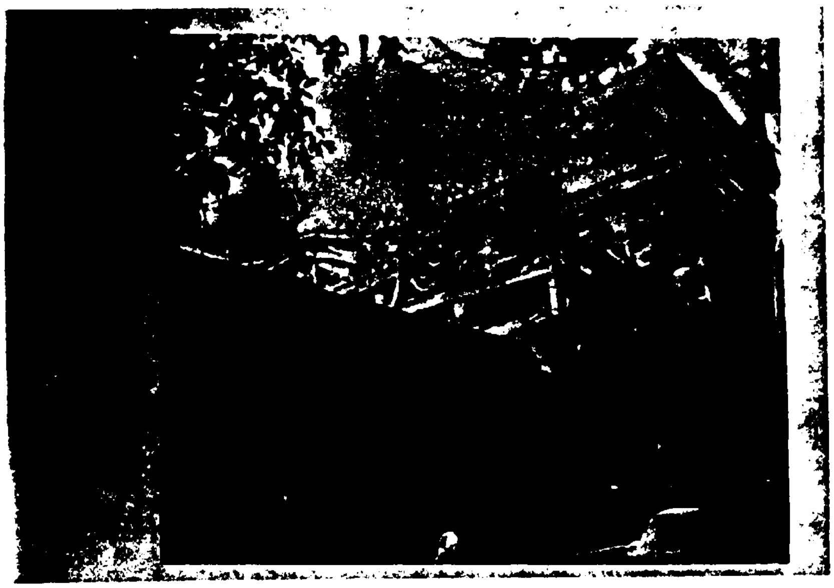

Figure 2.15. Building on Tehuantepec No. 12 (Photograph after International Masonry Institute, 1986)

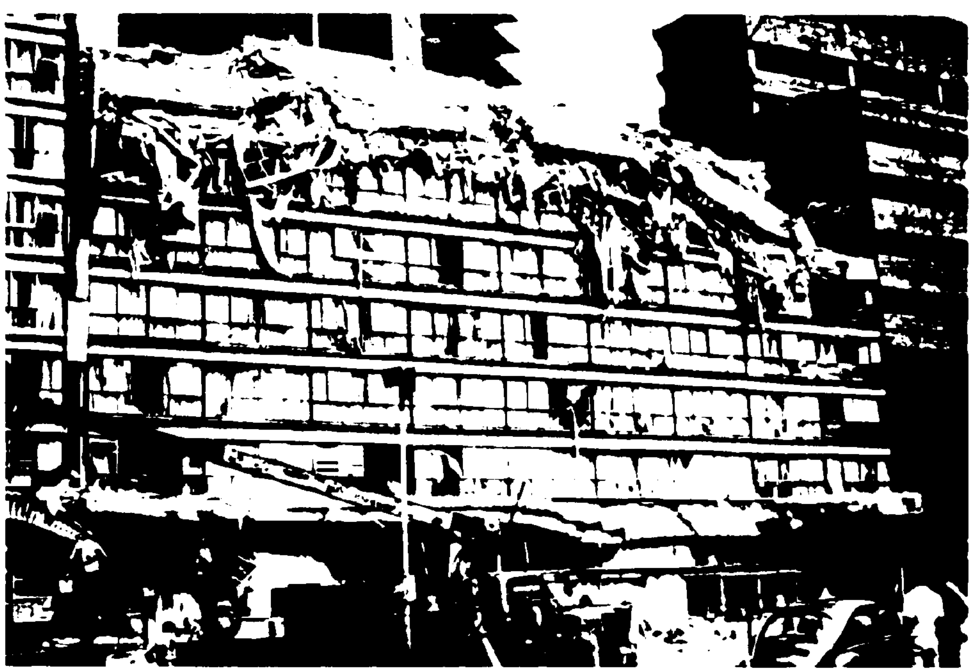

Figure 2.16. Building on Calle Roma (Hotel Continental)

Figure 2.17. Building on Fray Servando Teresa de Mier near Pino Suarez (photograph after International Masonry Institute, 1986)

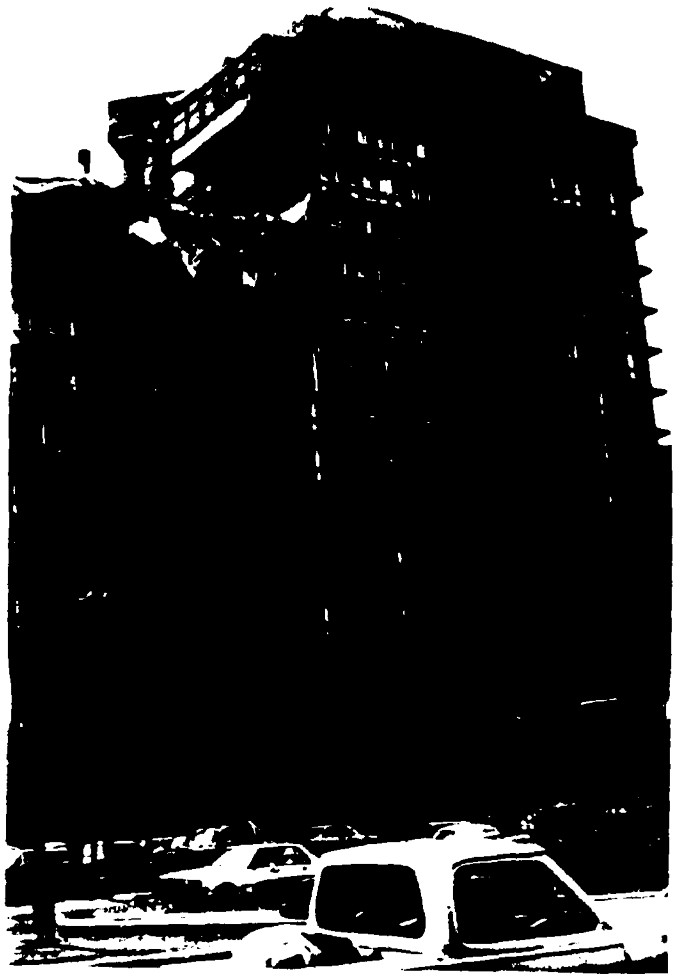

Figure 2.13. Building on Paseo de la Reforma (Hotel Continental)

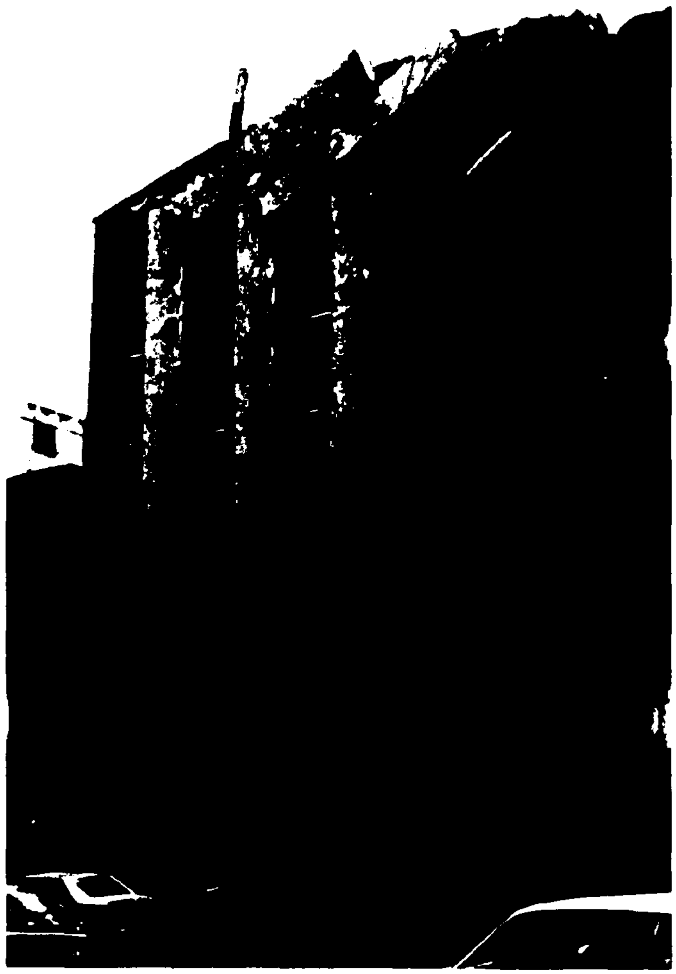

Figure 2.19. Building on Londres No. 13

Figure 2.20. Building on Ave. Morelos No. 98

Figure 2.21. Building on Liverpool and Berlin

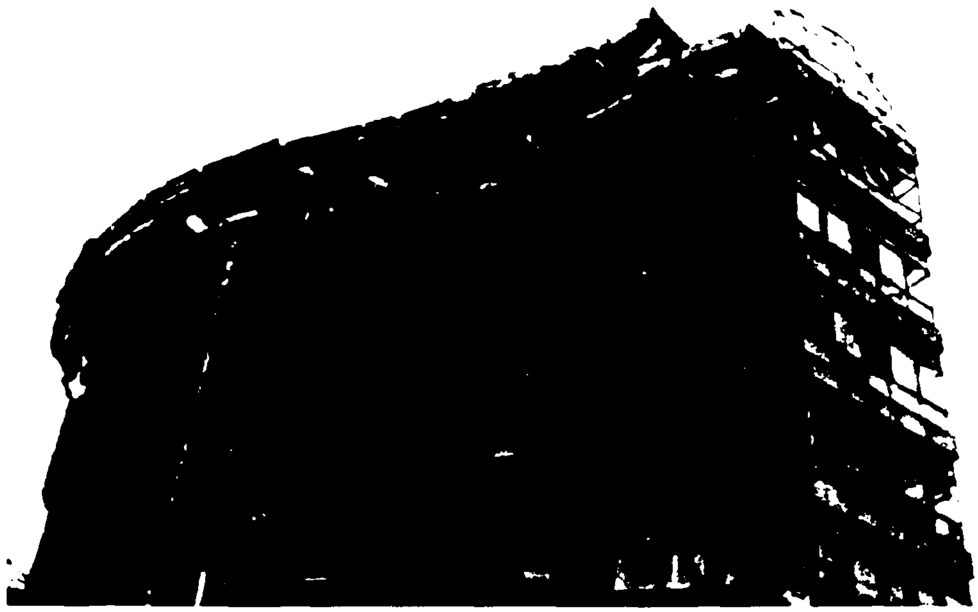

Figure 2.22. Building on Ave. de los Insurgentes and Guanajuato

Figure 2.23 Building on Fray Servando Teresa de Mier No. 154
(photograph after D. Mitchel, 1987)

Figure 2.24 Building on Ave. 20 de Noviembre near Regina (photograph after D. Mitchel, 1987)

Figure 2.25 Building on Lázaro Cardenas No. 21 (photograph after R. Hanson, 1986)

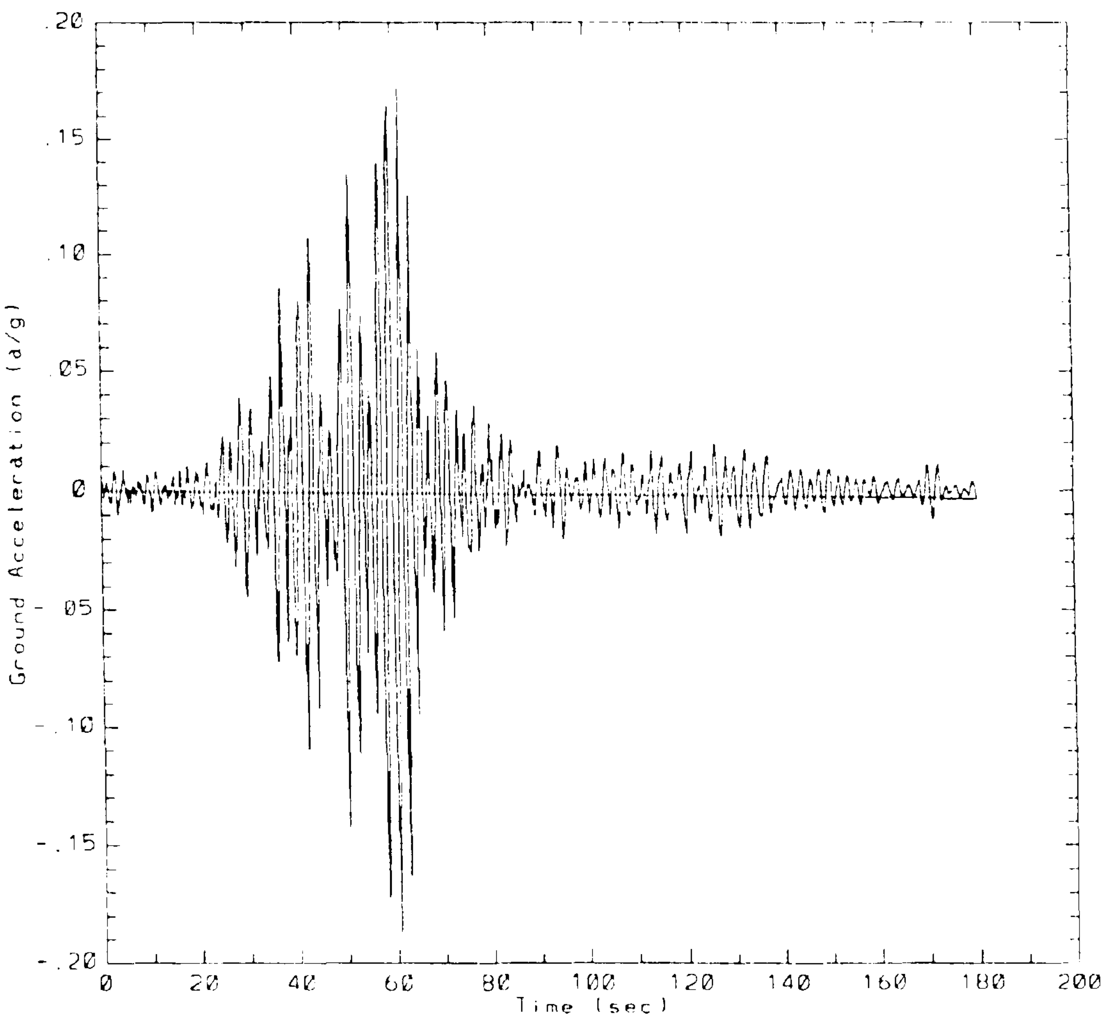

Figure 3.1. S60E component of SCT, September 19, 1985, ground acceleration record

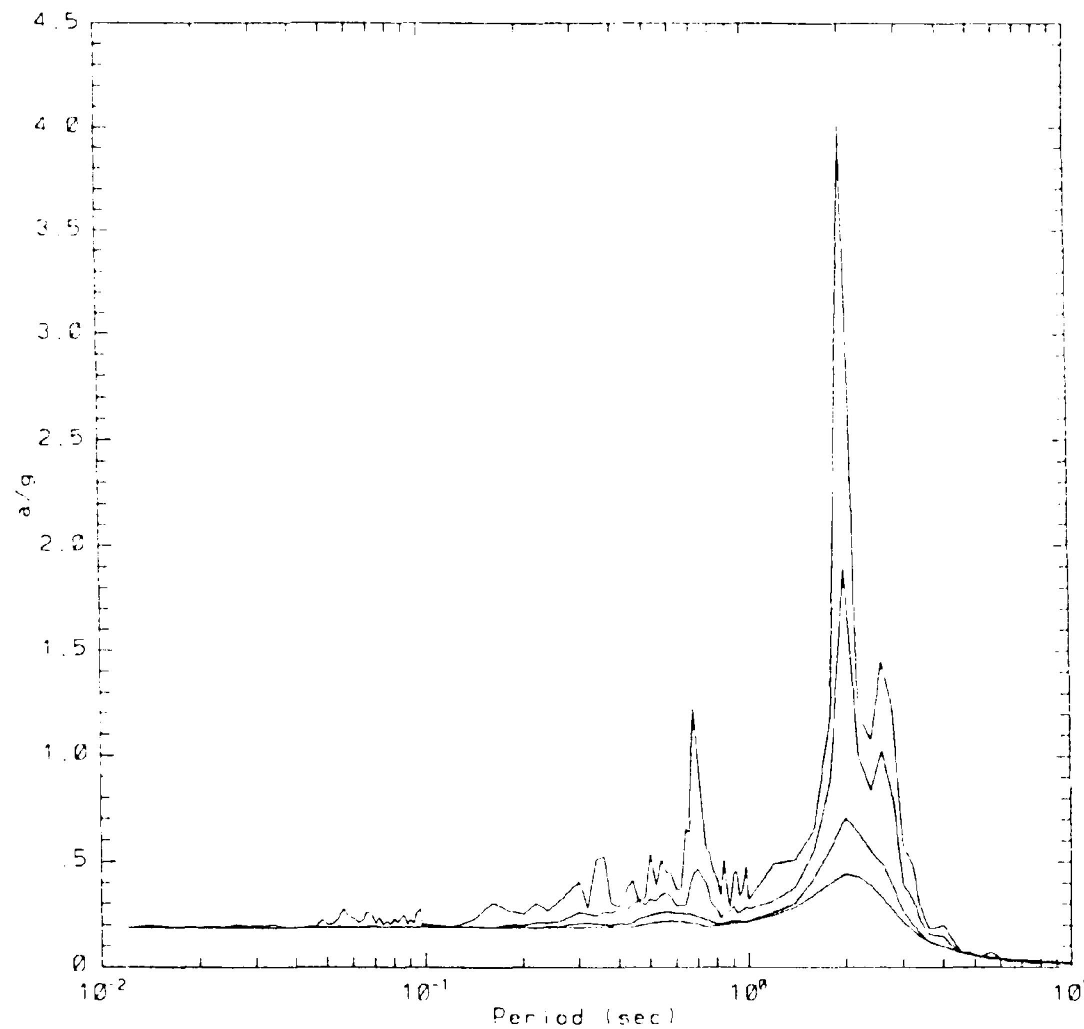

Figure 3.2. Acceleration response spectra for 0, 2, 10, and 20 percent damping of S60E component of SCT ground acceleration record

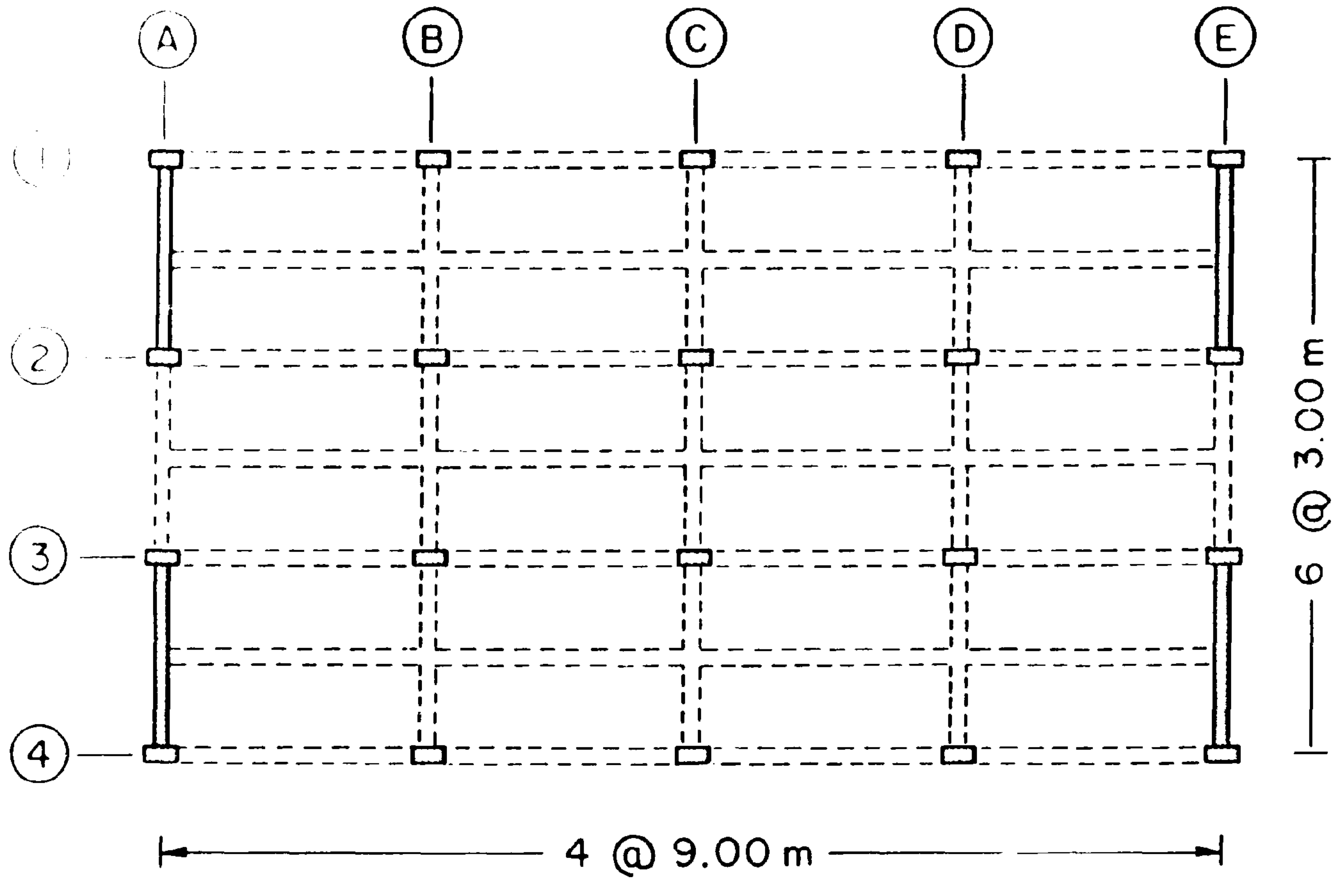

Figure 3.3. Floor plan of building in simulation study

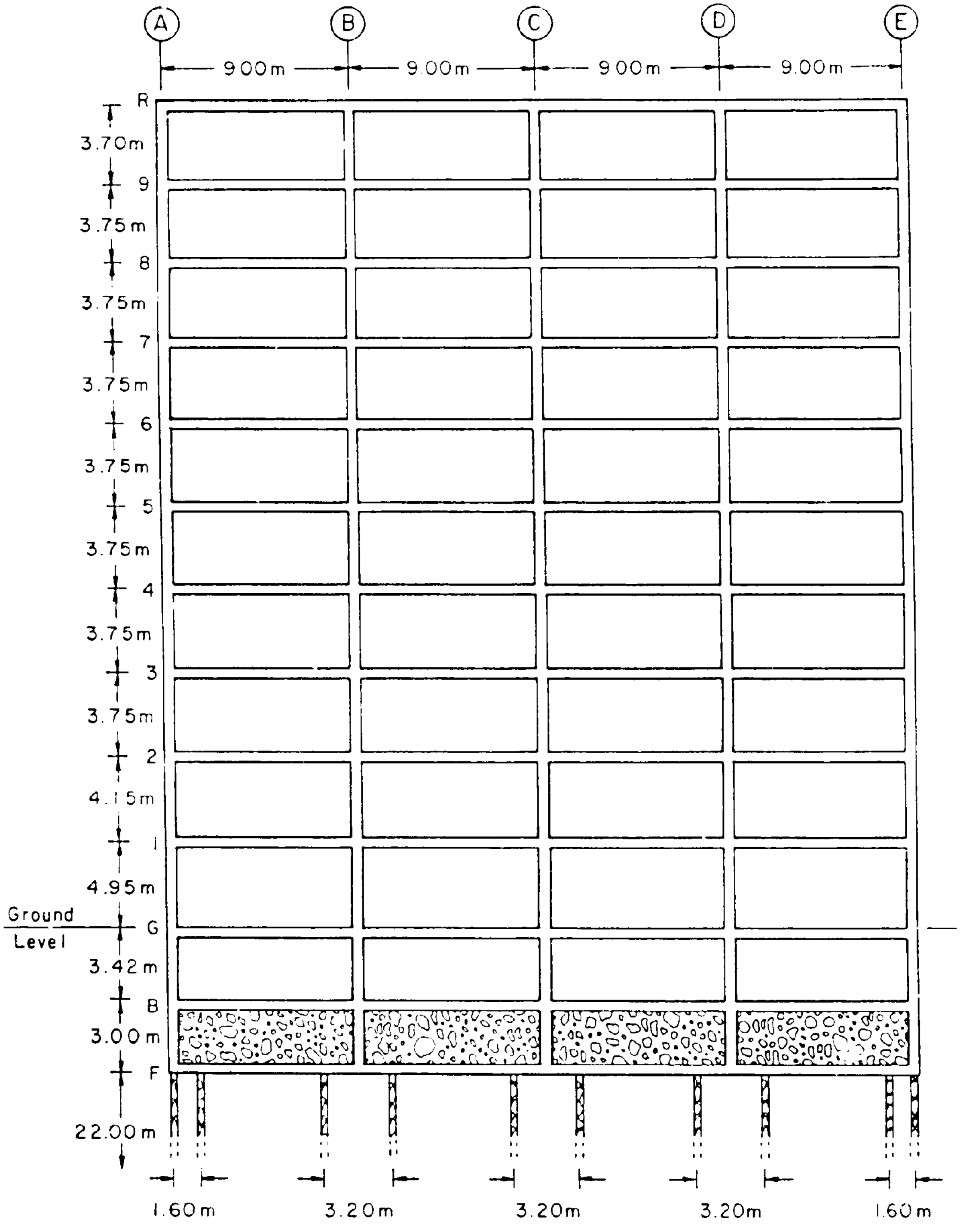

Figure 3.4. Longitudinal elevation (Section 3-3) of building in simulation study

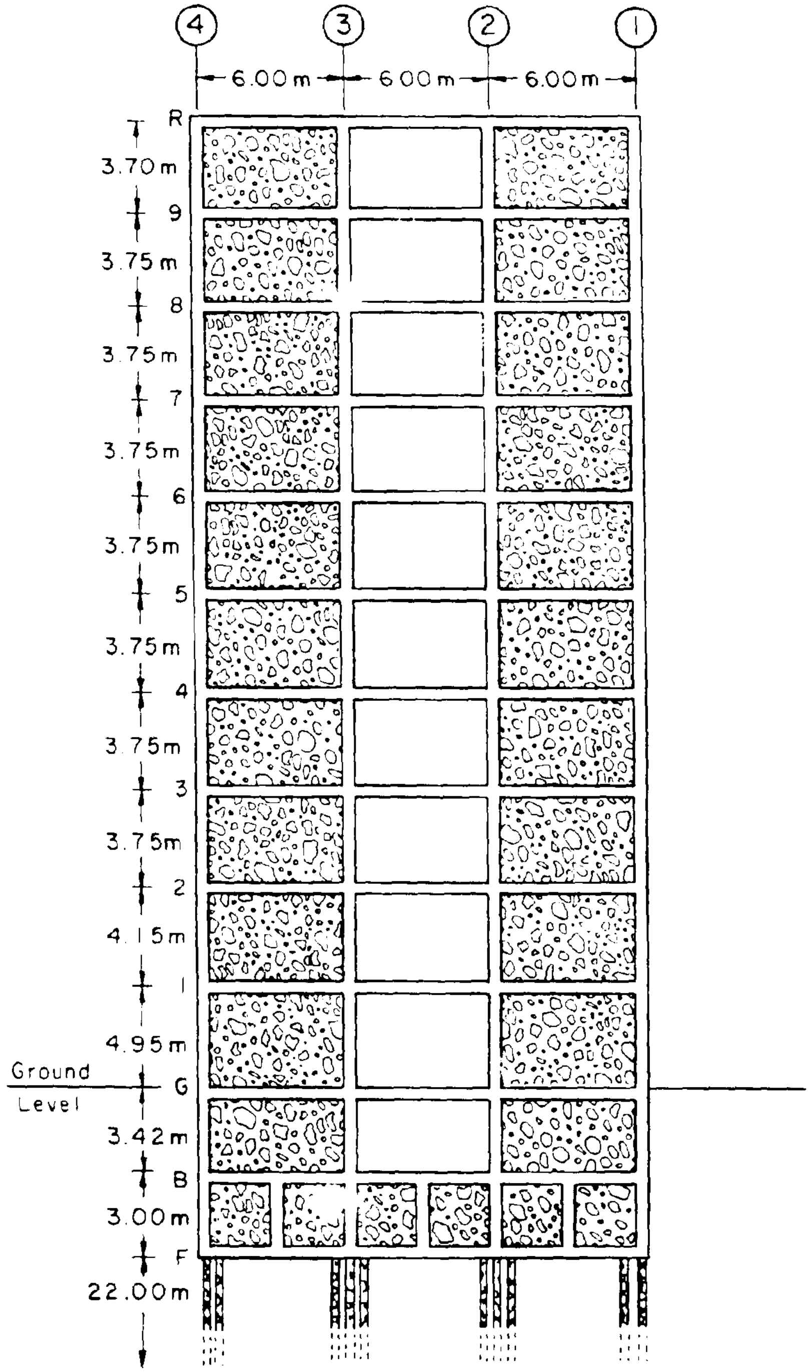

Figure 3.5. Transverse elevation (Section A-A) of building in simulation study

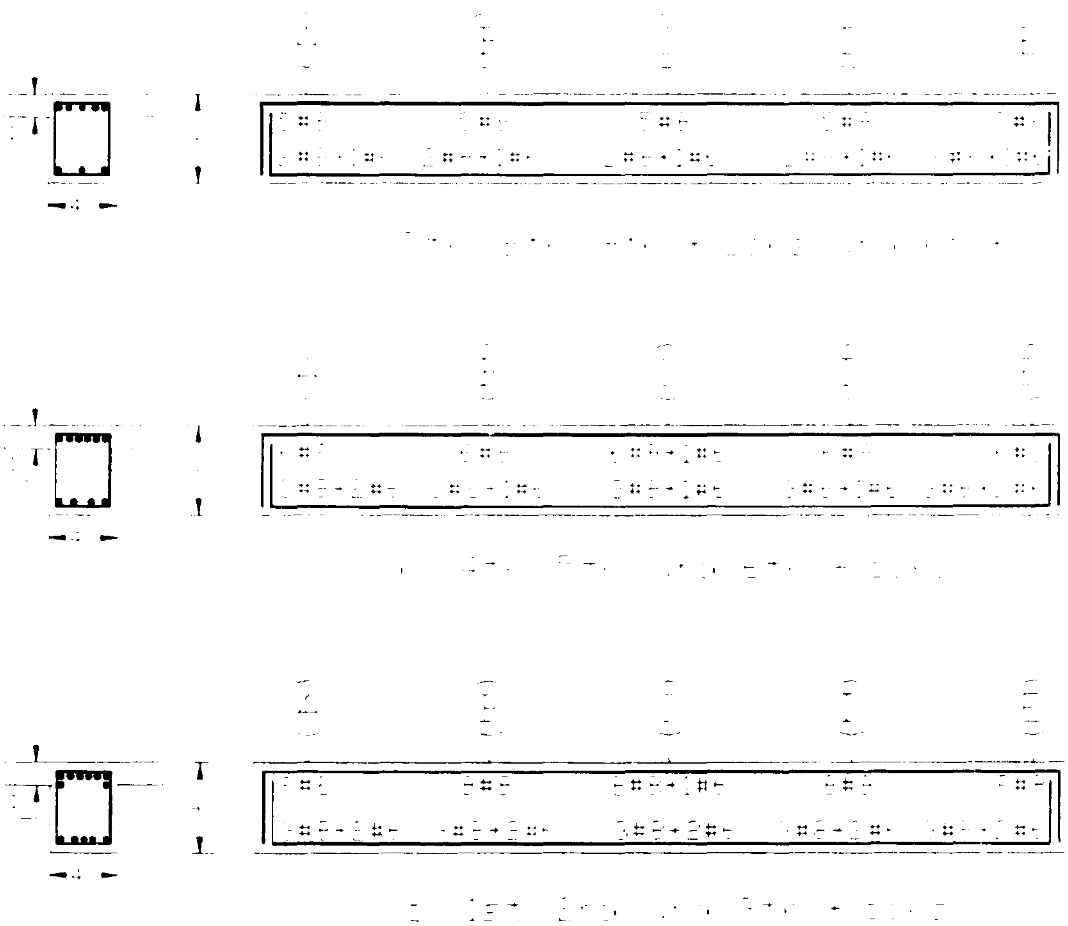

Figure 3.6. Cross sections and reinforcement of beams of interior longitudinal frame of original STC building (dimensions in centimeters)

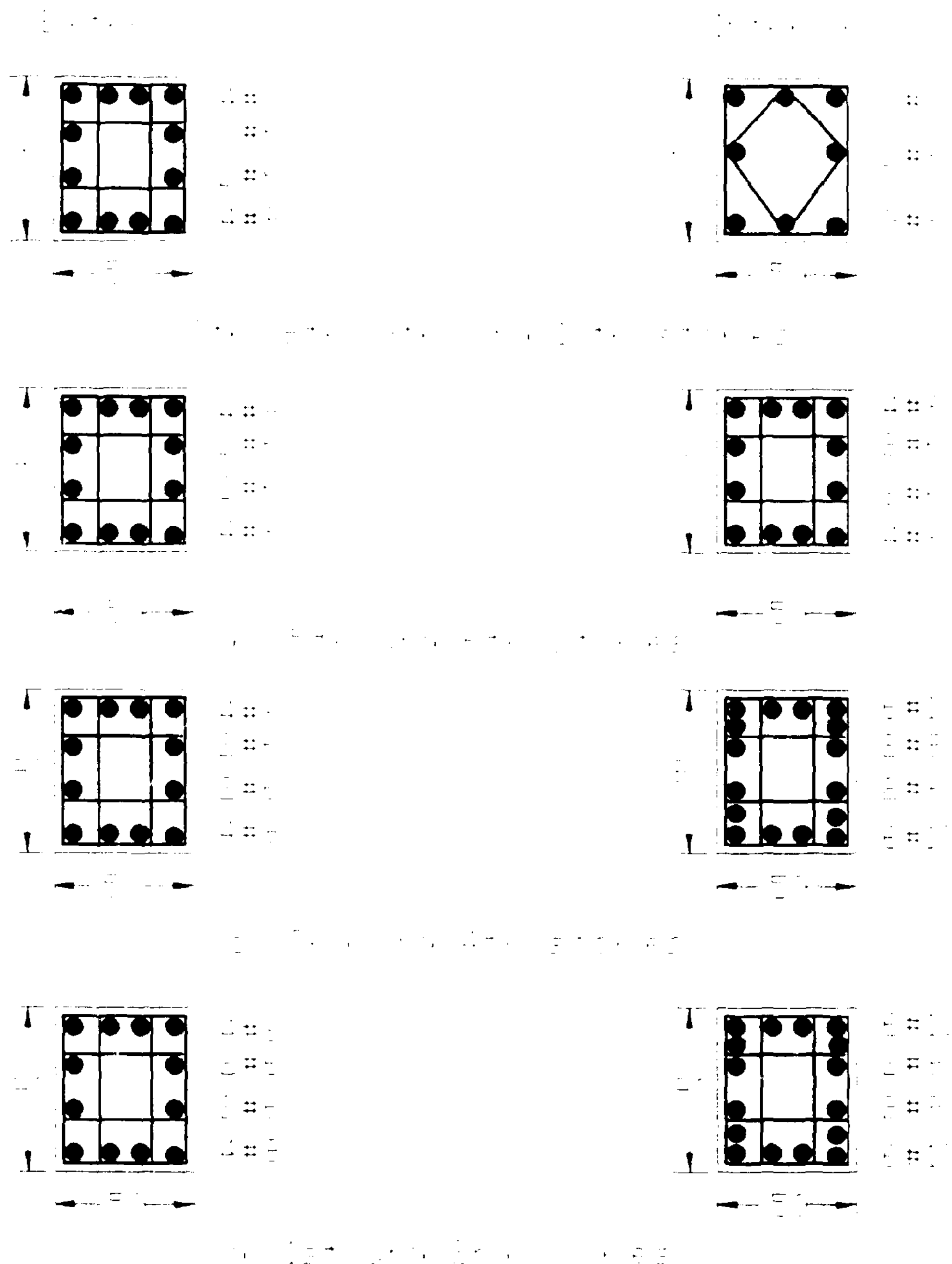

Figure 3.7. Cross sections and reinforcement of columns in interior longitudinal frame of original STC building (dimensions in centimeters)

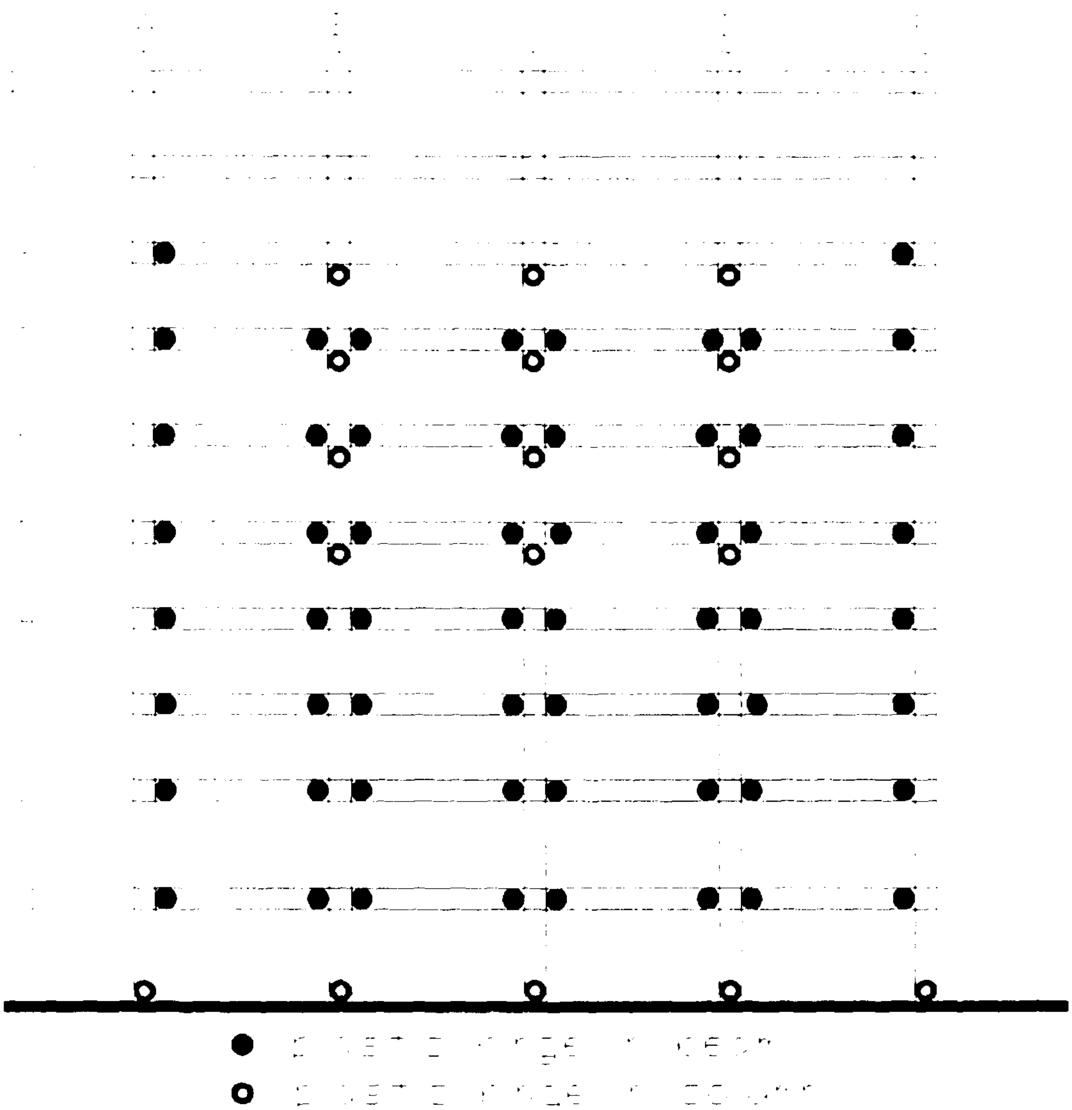

Figure 3.8. Plastic hinges in interior longitudinal frame of original STC building after 70 sec. of the SCT, S60E, ground motion

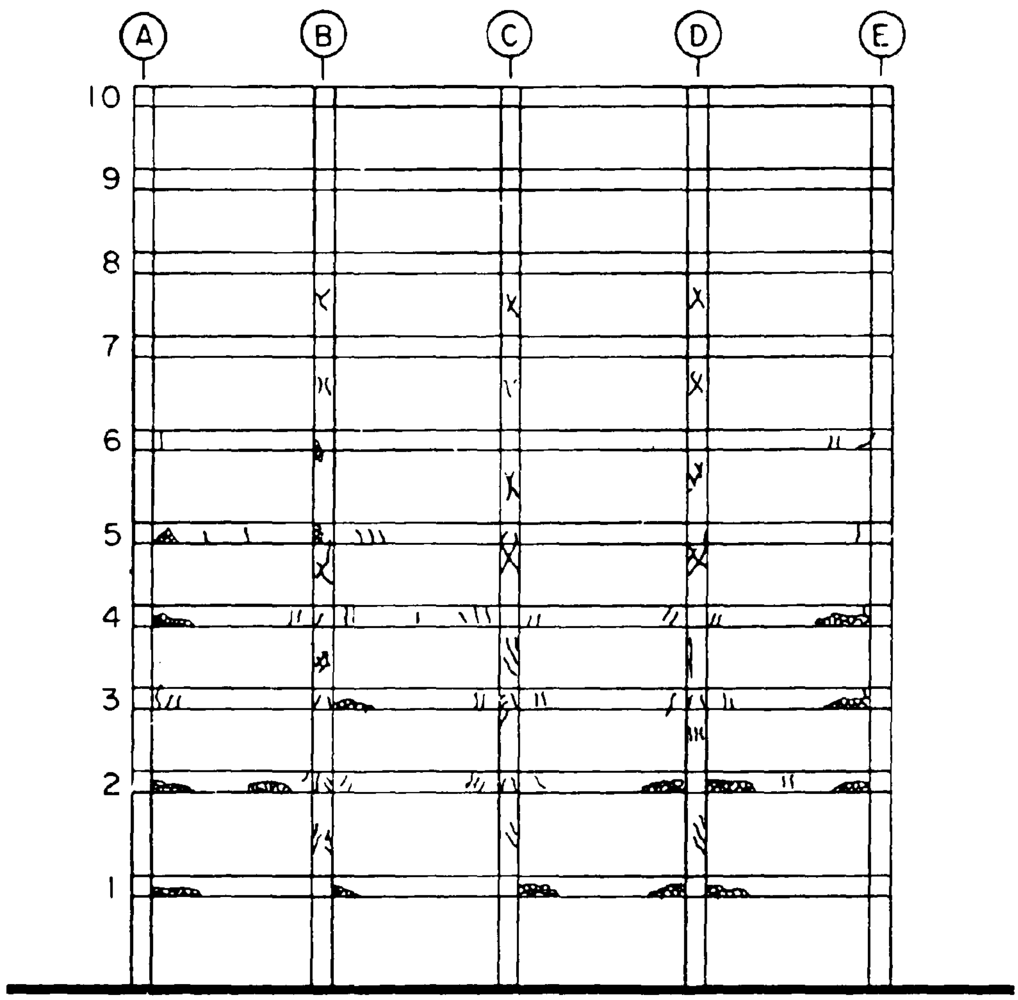

Figure 3.9. Damage sustained by interior longitudinal frame of STC building during the earthquake of September 19, 1985 (after Meli and López, 1986)

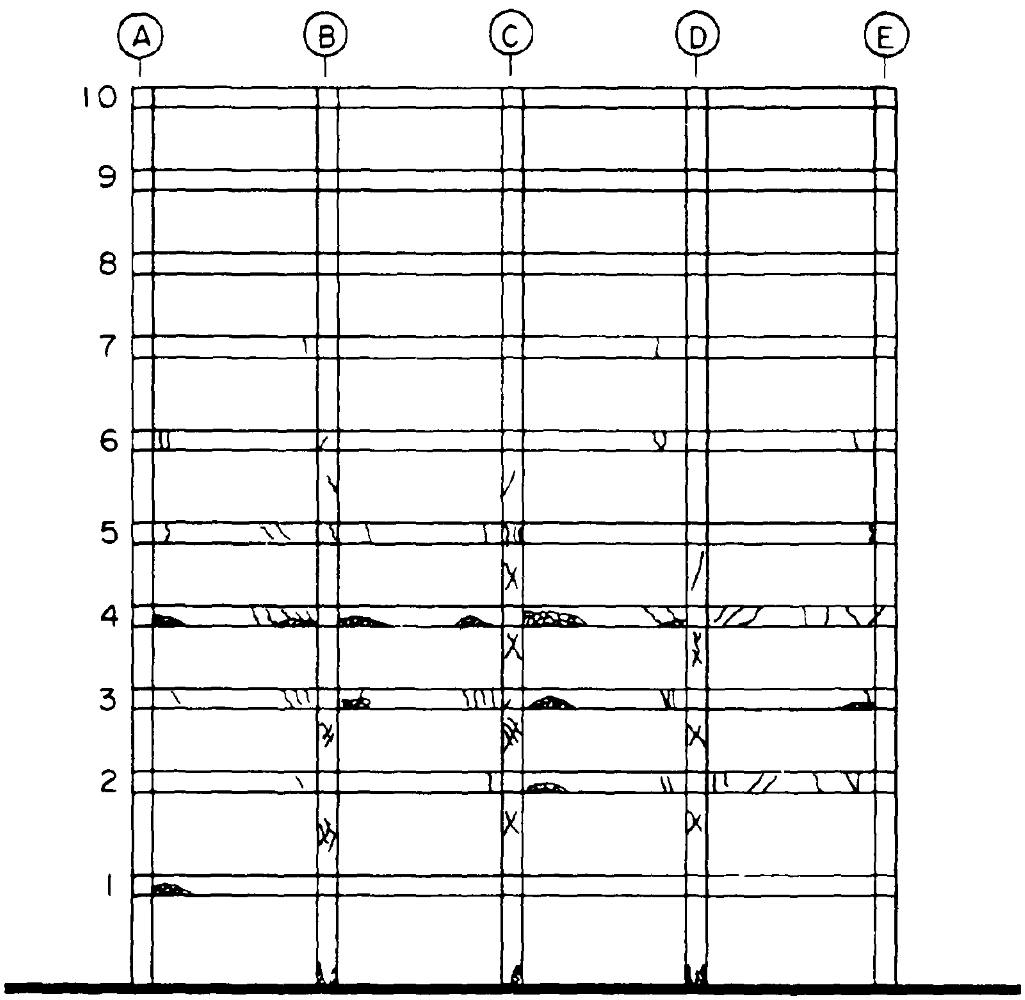

Figure 3.10. Damage sustained by exterior longitudinal frame of STC building during the earthquake of September 19, 1985 (after Meli and López, 1986)

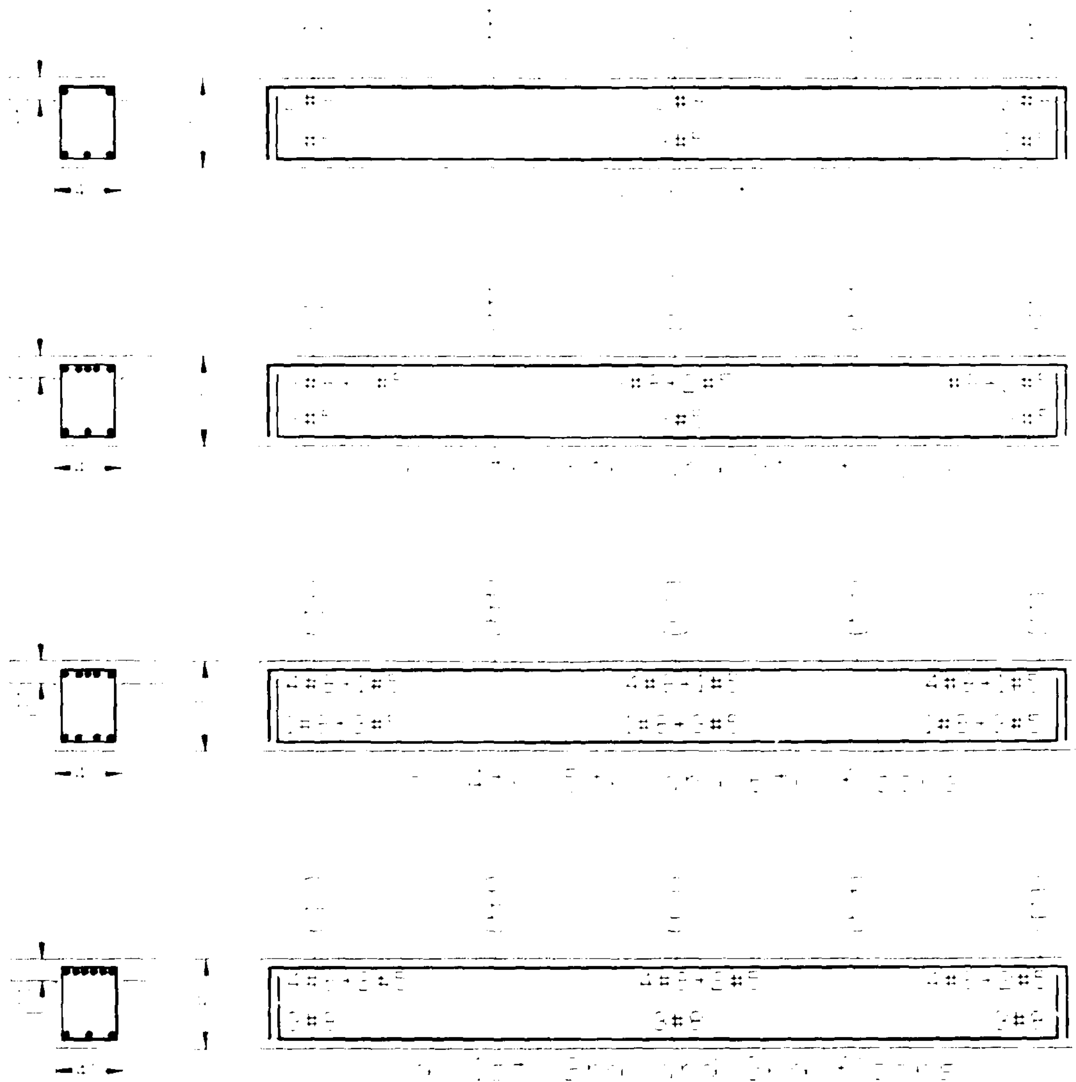

Figure 3.11. Cross sections and reinforcement of beams of interior longitudinal frame of designed 10-story building (dimensions in centimeters)

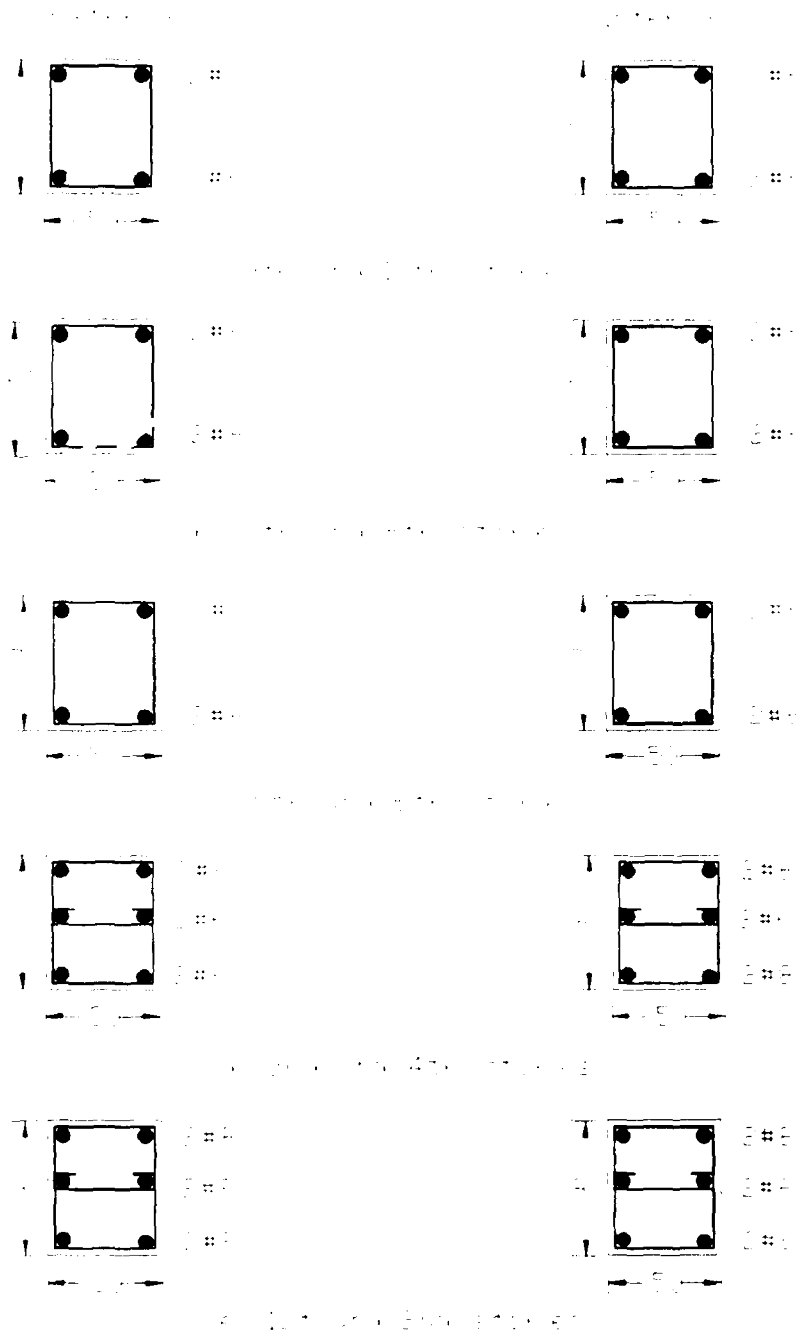

Figure 3.12. Cross sections and reinforcement of columns of interior longitudinal frame of designed 10-story building (dimensions in centimeters)

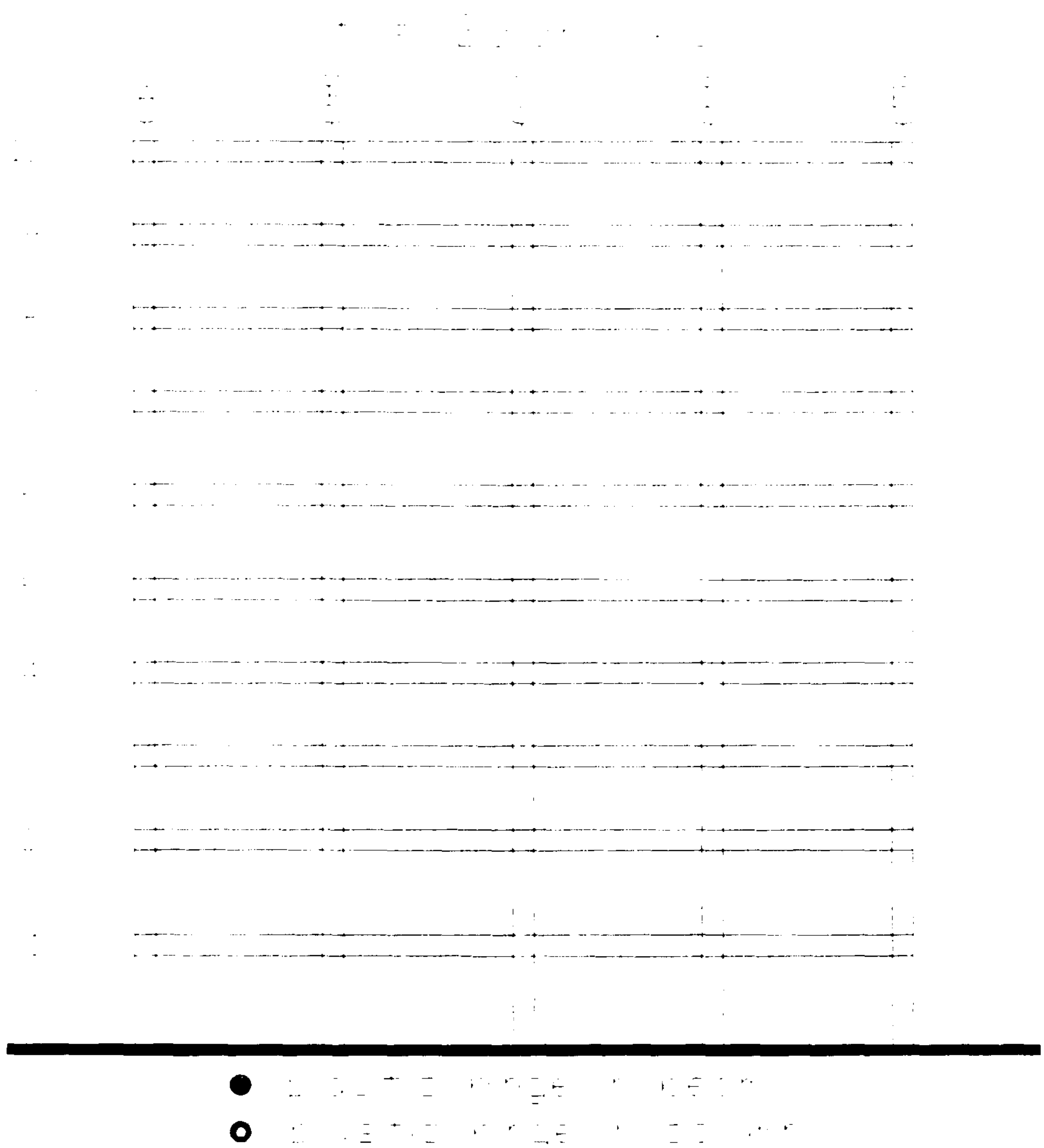

Figure 3.13. Plastic hinges in interior longitudinal frame of designed 10-story building after 23.36 sec. of the SCT, S60E, ground motion

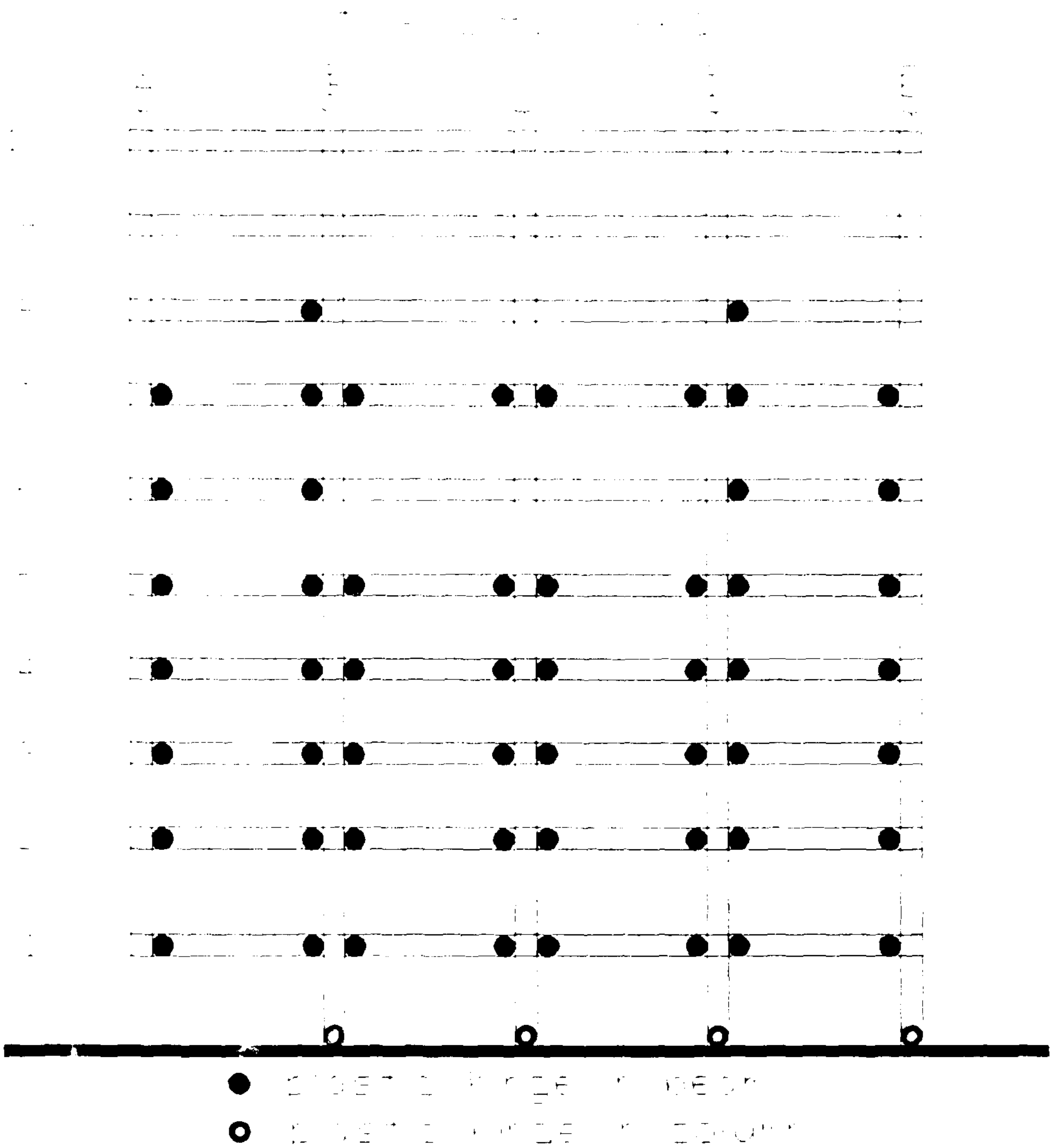

Figure 3.14. Plastic hinges in interior longitudinal frame of designed 10-story building after 29.20 sec. of the SCT, S60E, ground motion

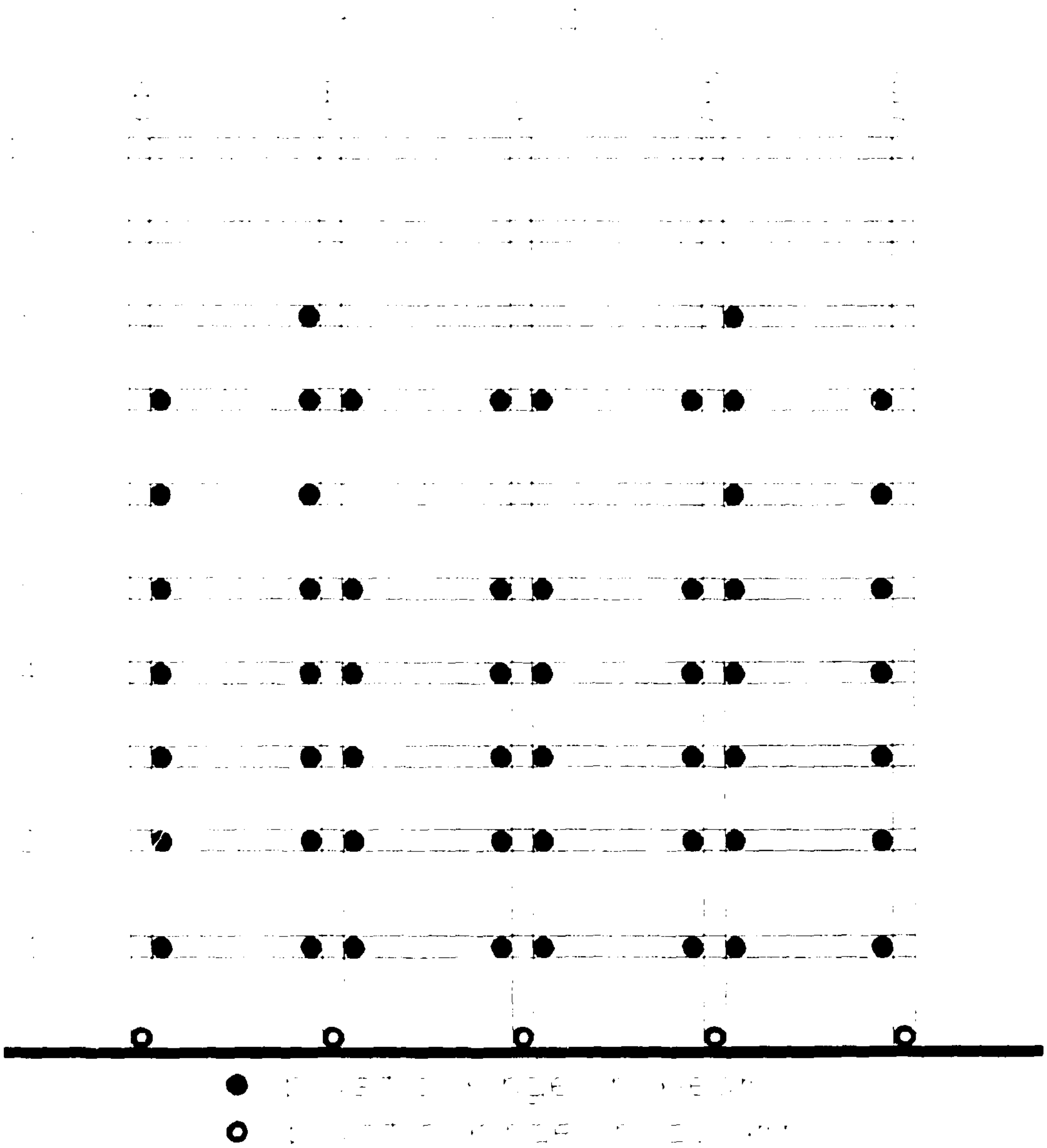

Figure 3.15. Plastic hinges in interior longitudinal frame of designed 10-story building after 35.04 sec. of the SCT, S60E, ground motion

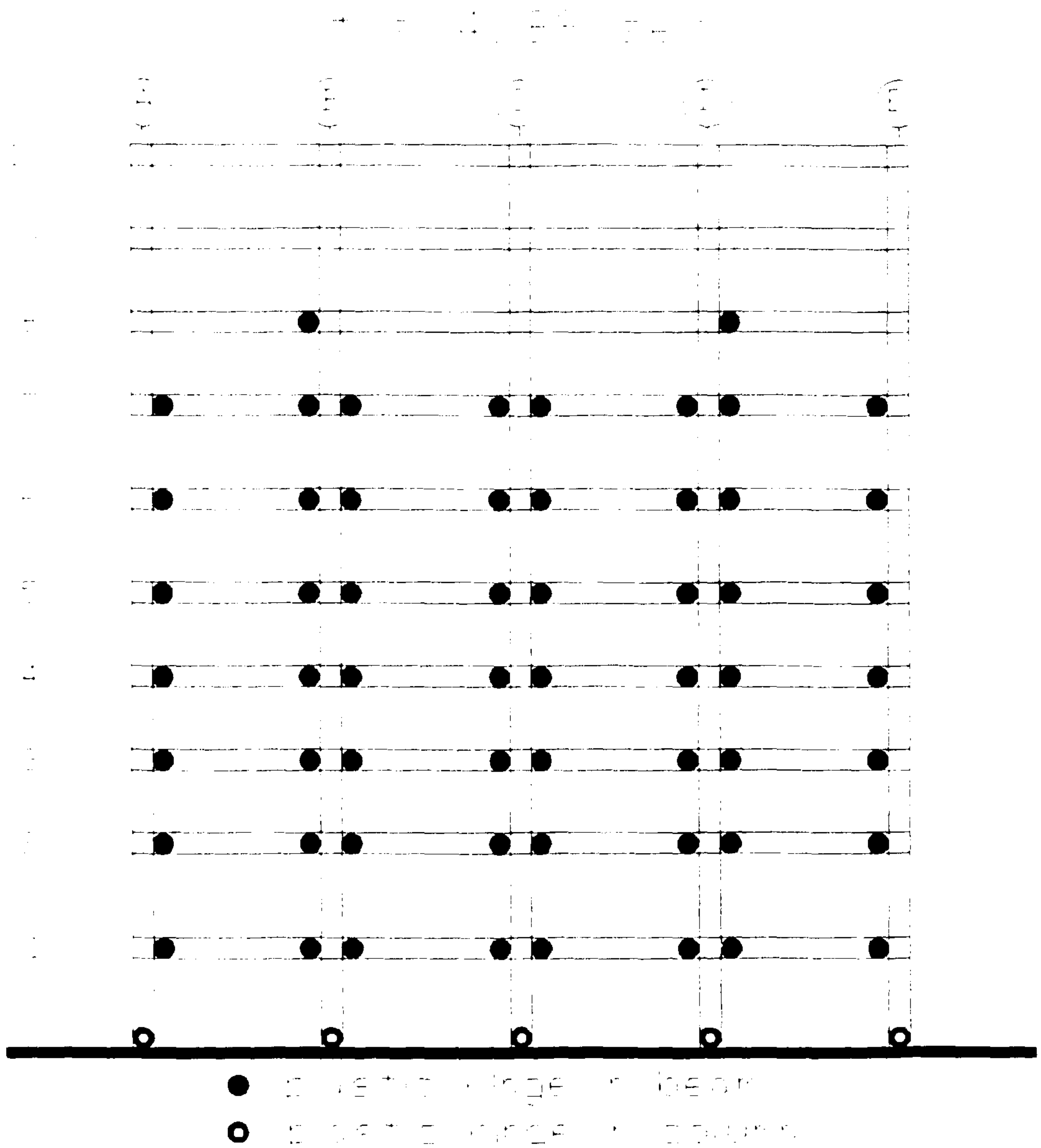

Figure 3.16. Plastic hinges in interior longitudinal frame of designed 10-story building after 40.88 sec. of the SCT, S60E, ground motion

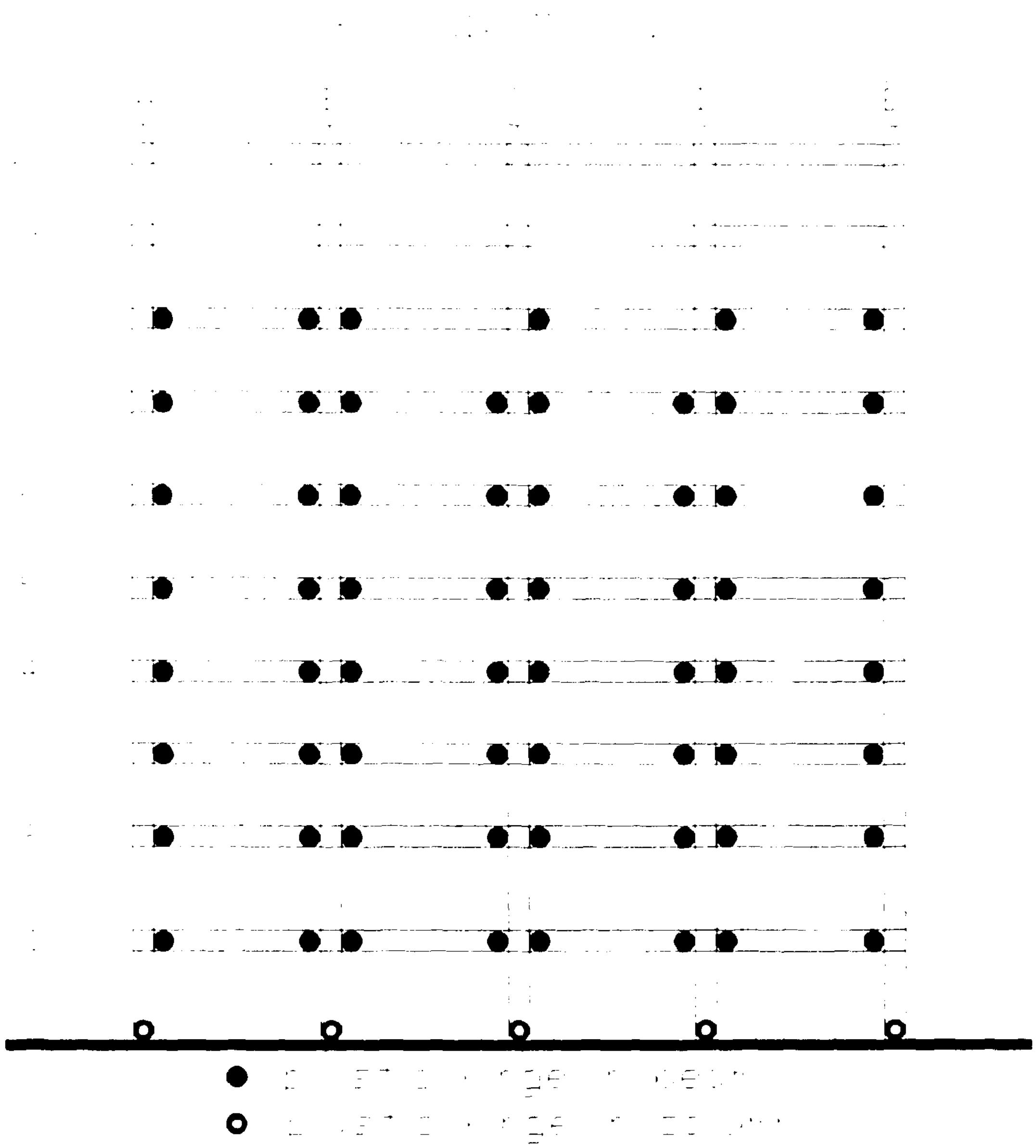

Figure 3.17. Plastic hinges in interior longitudinal frame of designed 10-story building after 46.72 sec. of the SCT, S60E, ground motion

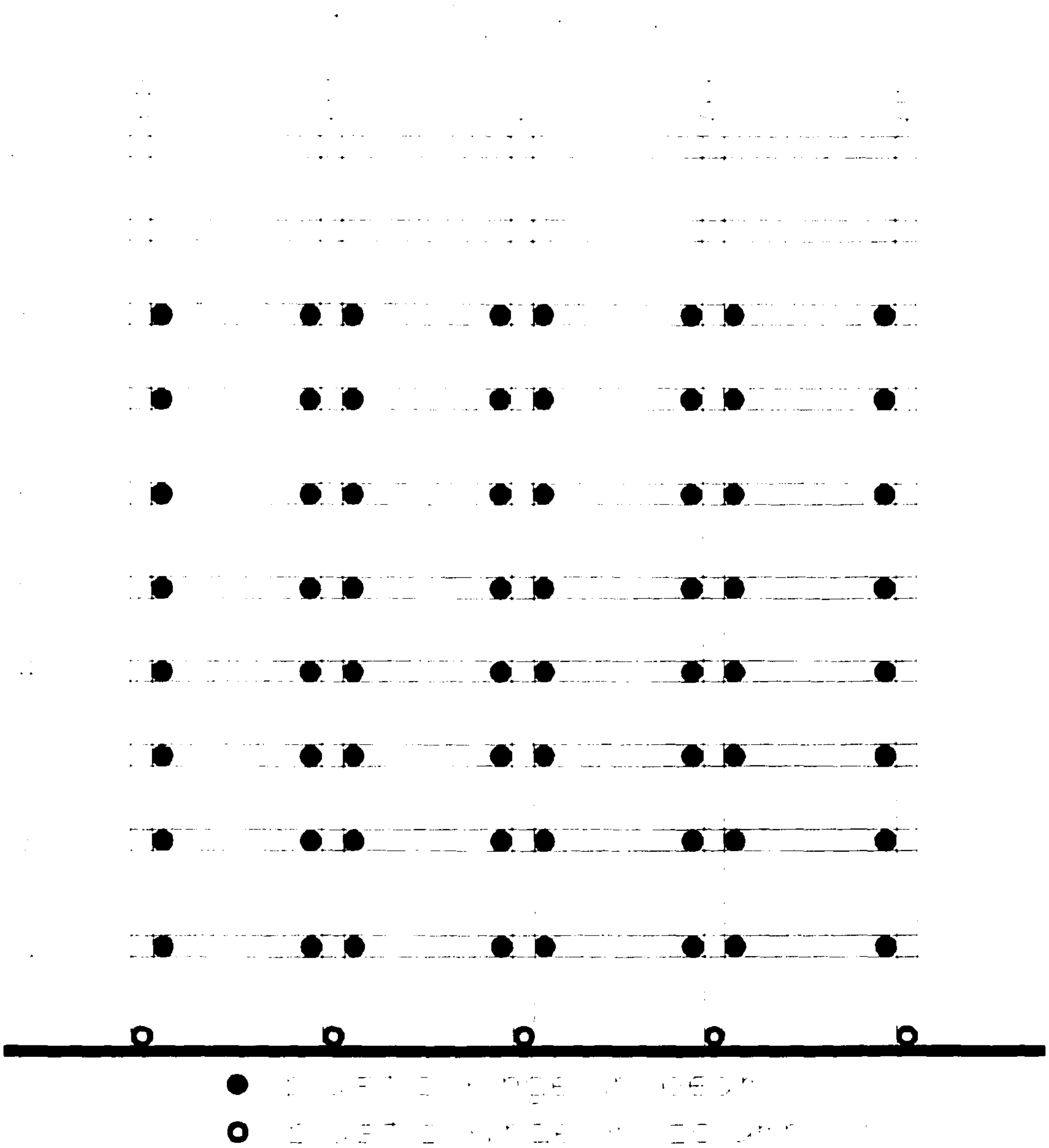

Figure 3.18. Plastic hinges in interior longitudinal frame of designed 10-story building after 52.56 sec. of the SCT, S60E, ground motion

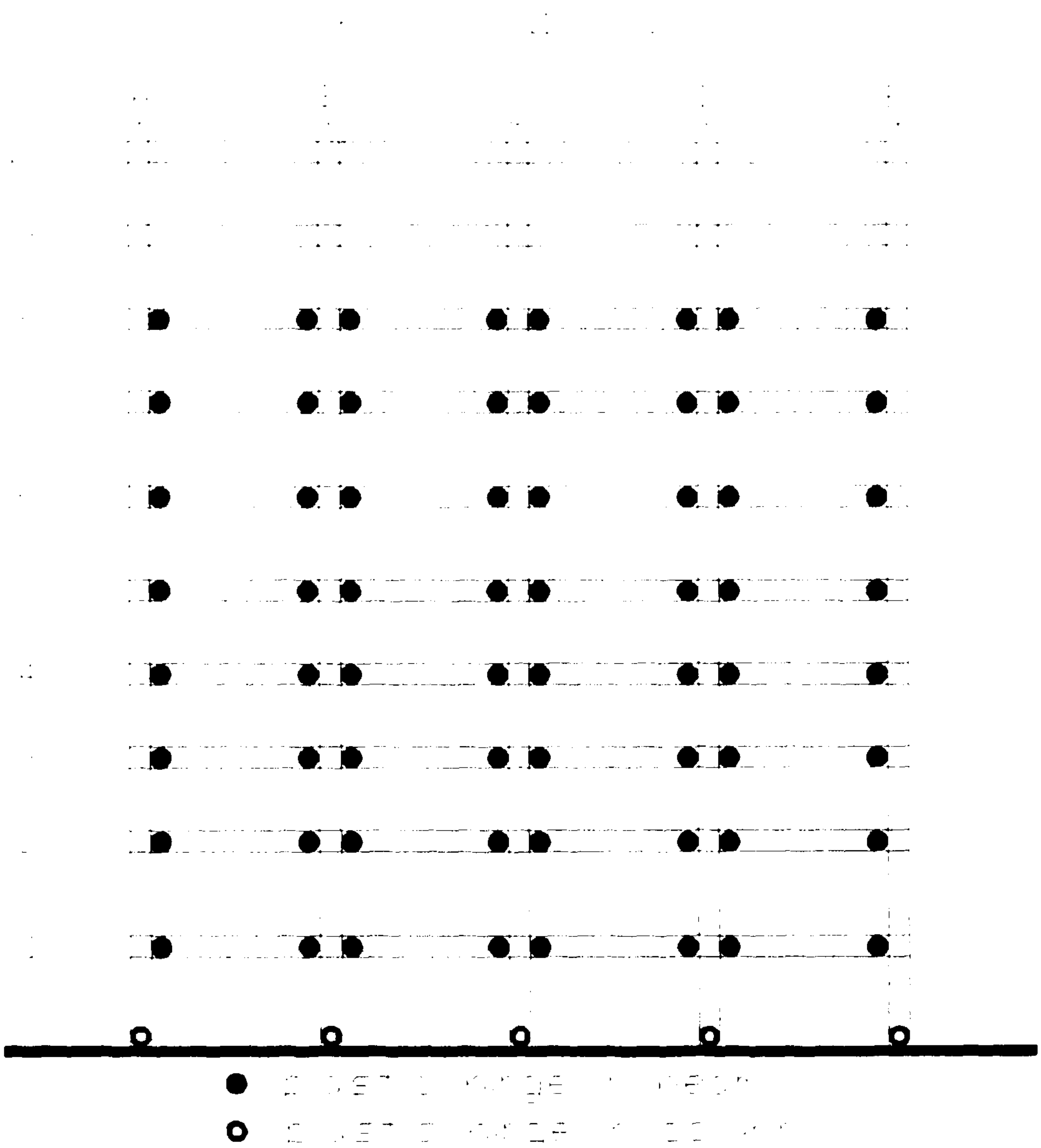

Figure 3.19. Plastic hinges in interior longitudinal frame of designed 10-story building after 58.40 sec. of the SCT, S60E, ground motion

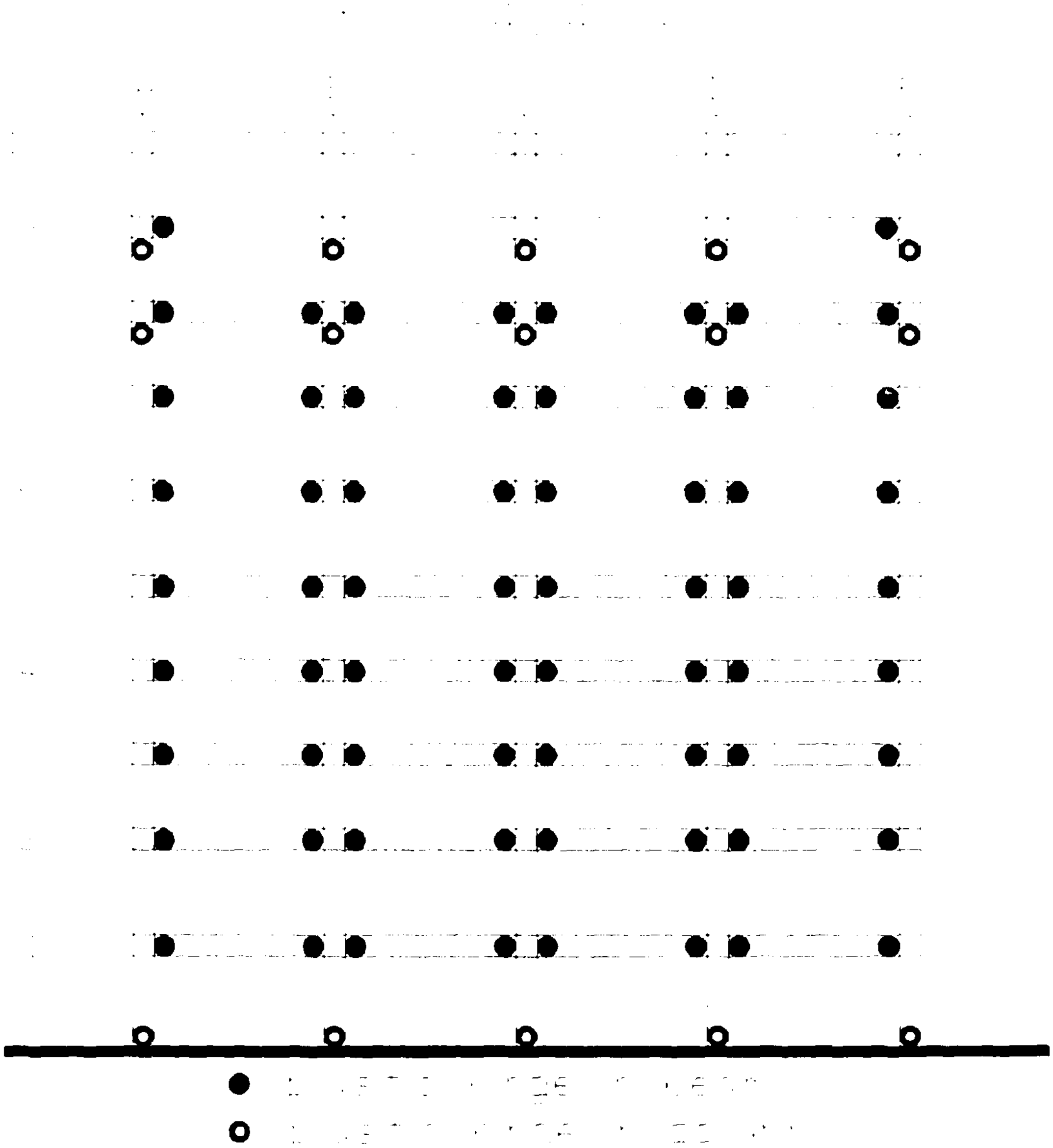

Figure 3.20. Plastic hinges in interior longitudinal frame of designed 10-story building after 64.24 sec. of the SCT, S60E, ground motion

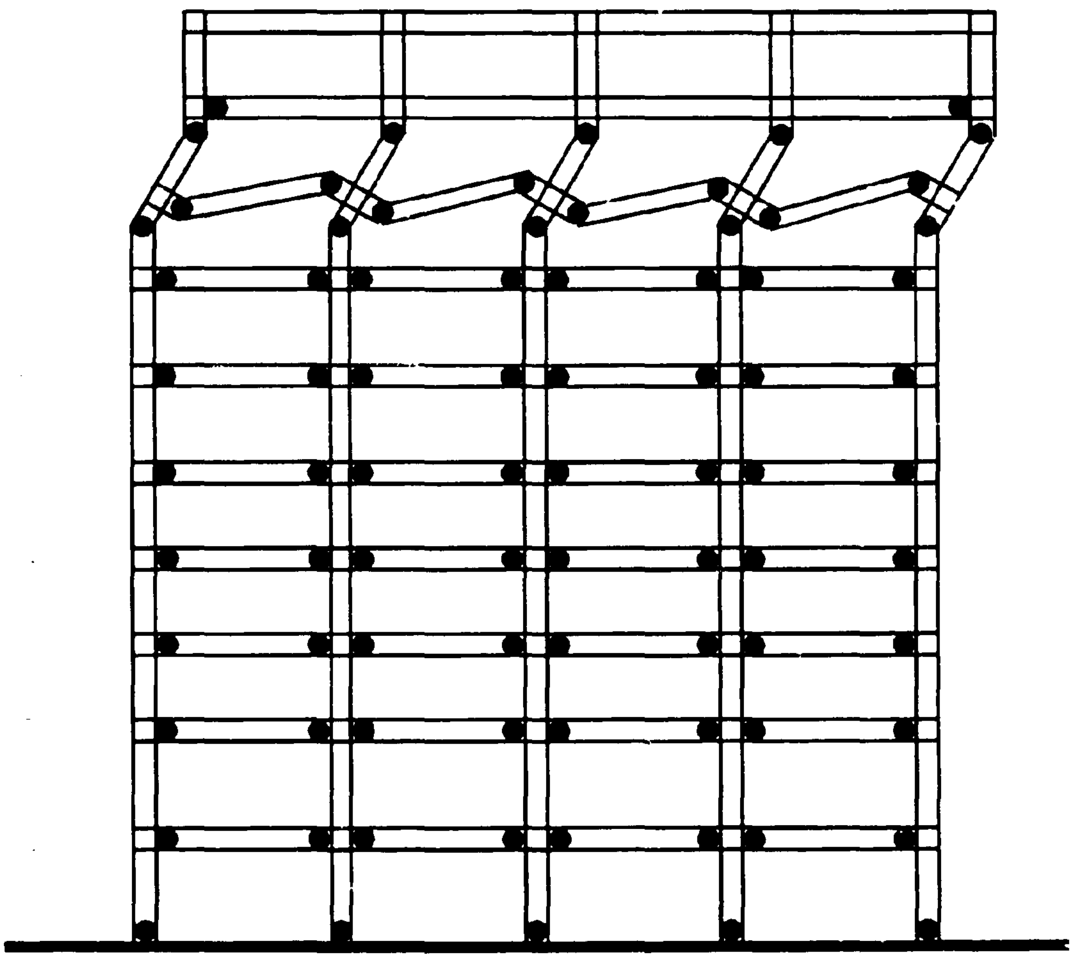

Figure 3.21. Upper floor failure mechanism in interior longitudinal frame of designed 10-story building

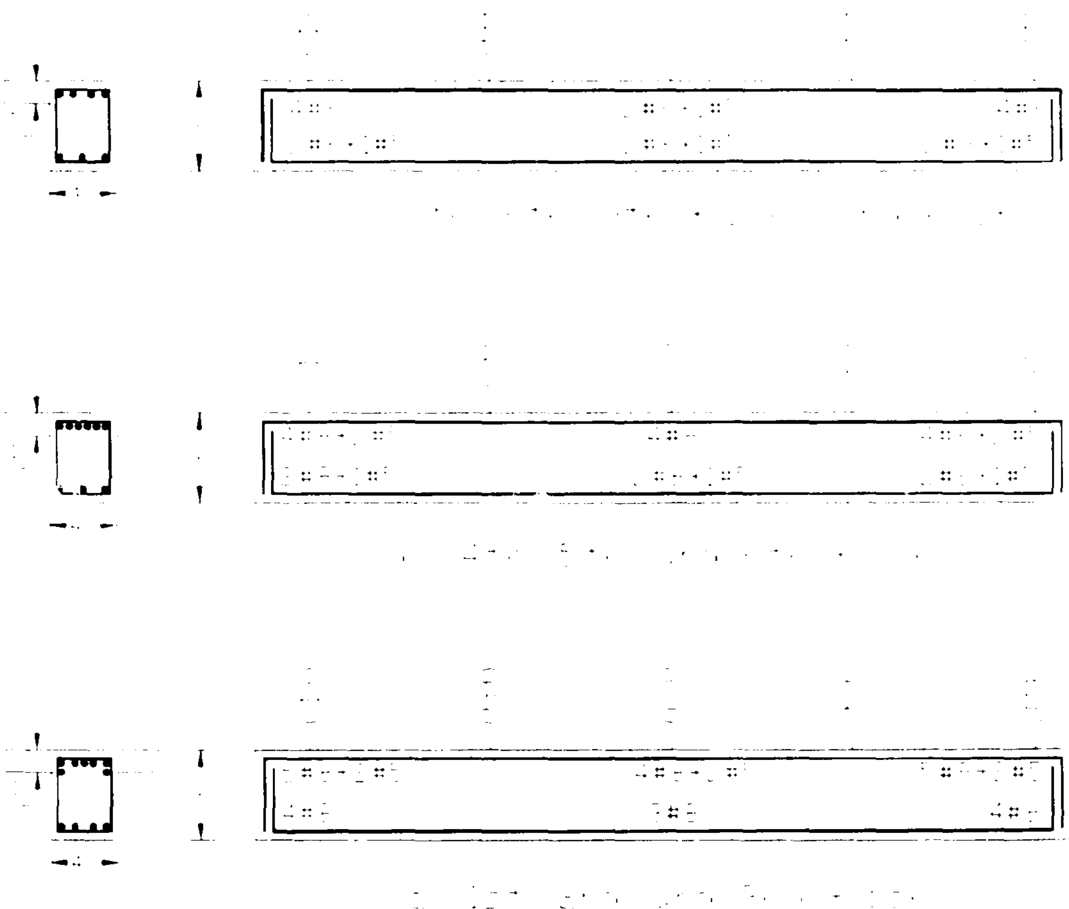

Figure 3.22. Cross sections and reinforcement of beams of interior longitudinal frame of redesigned 10-story building (dimensions in centimeters)

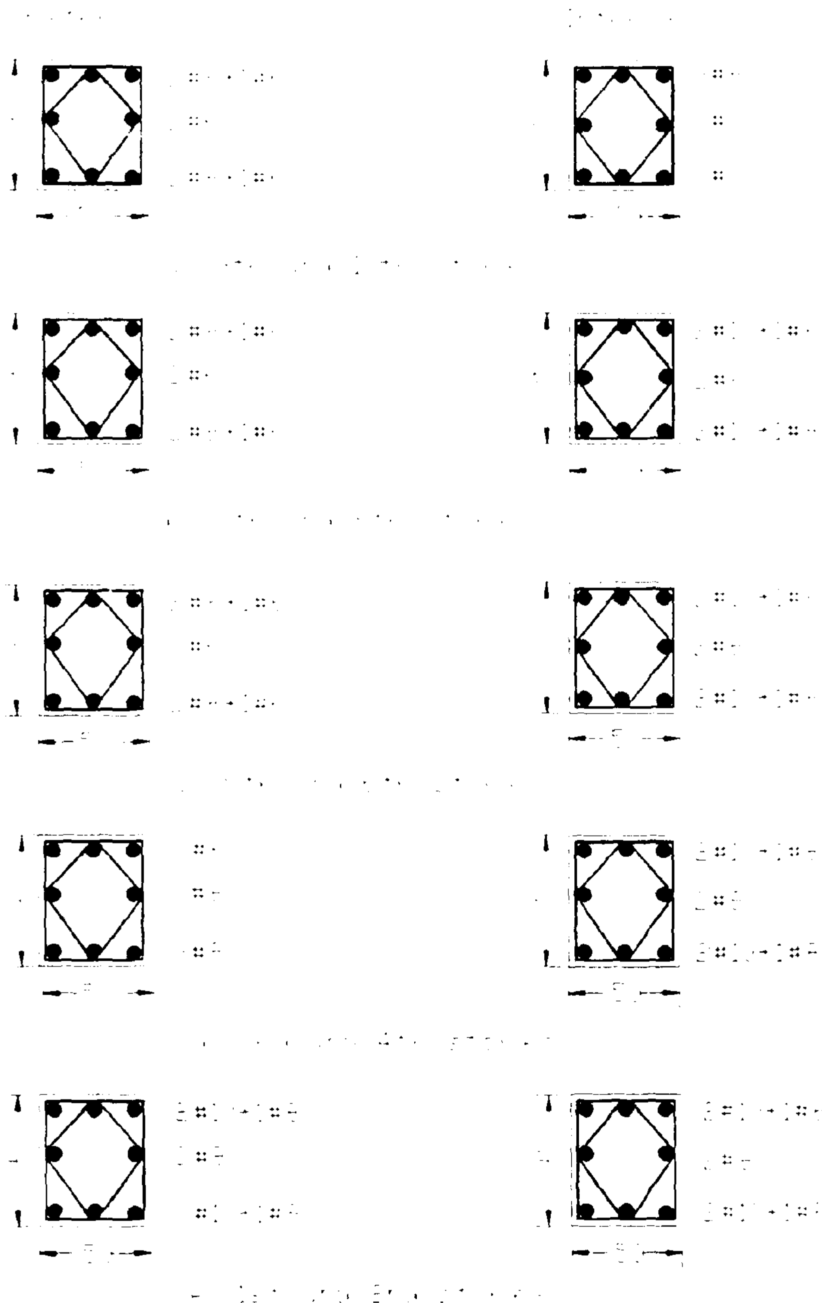

Figure 3.23. Cross sections and reinforcement of columns of interior longitudinal frame of redesign[illegible] [illegible]-story building (dimensions in centimeters)

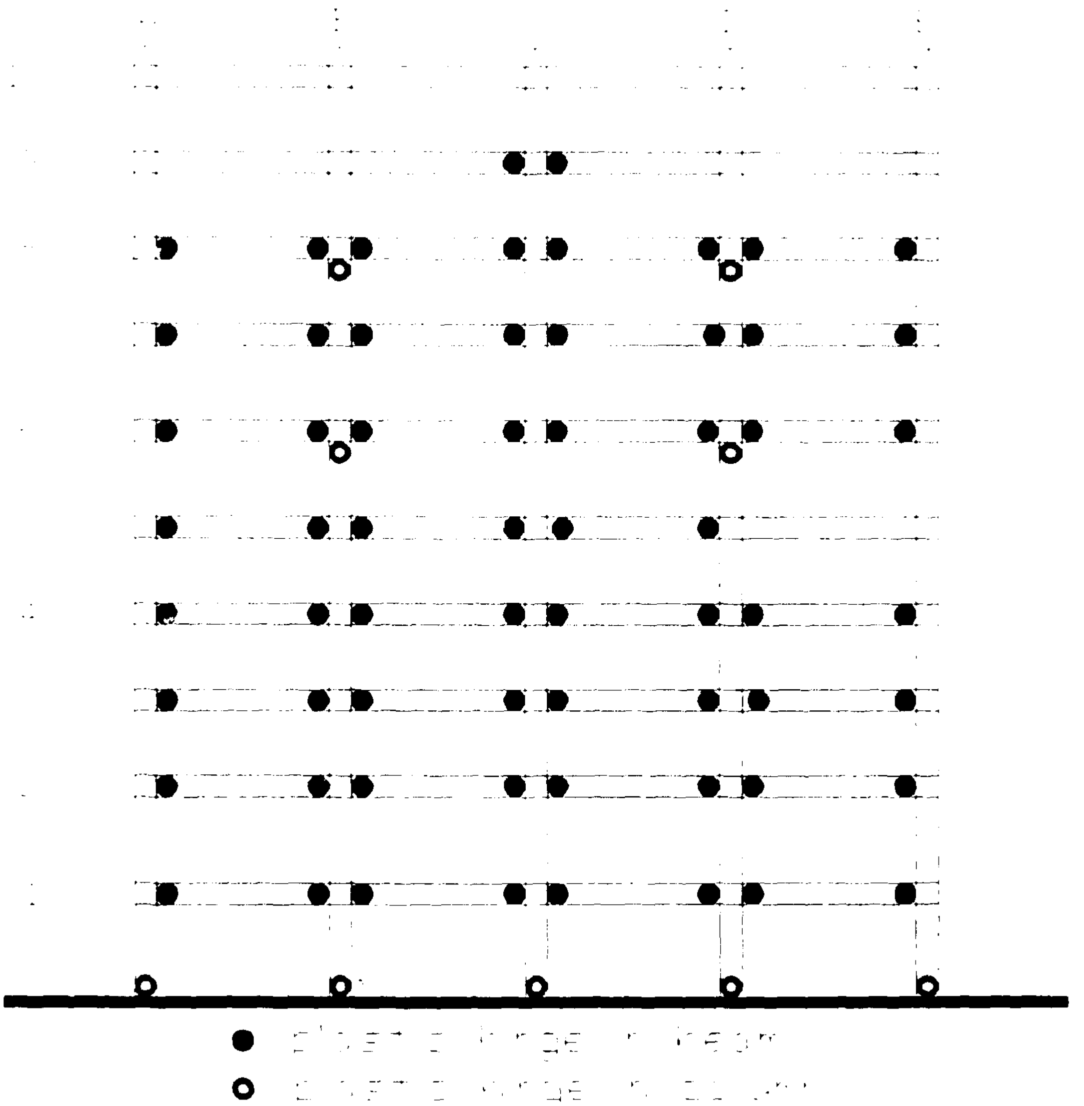

Figure 3.24. Plastic hinges in interior longitudinal frame of redesigned 10-story building after 70 sec. of the SCT, S60E, ground motion

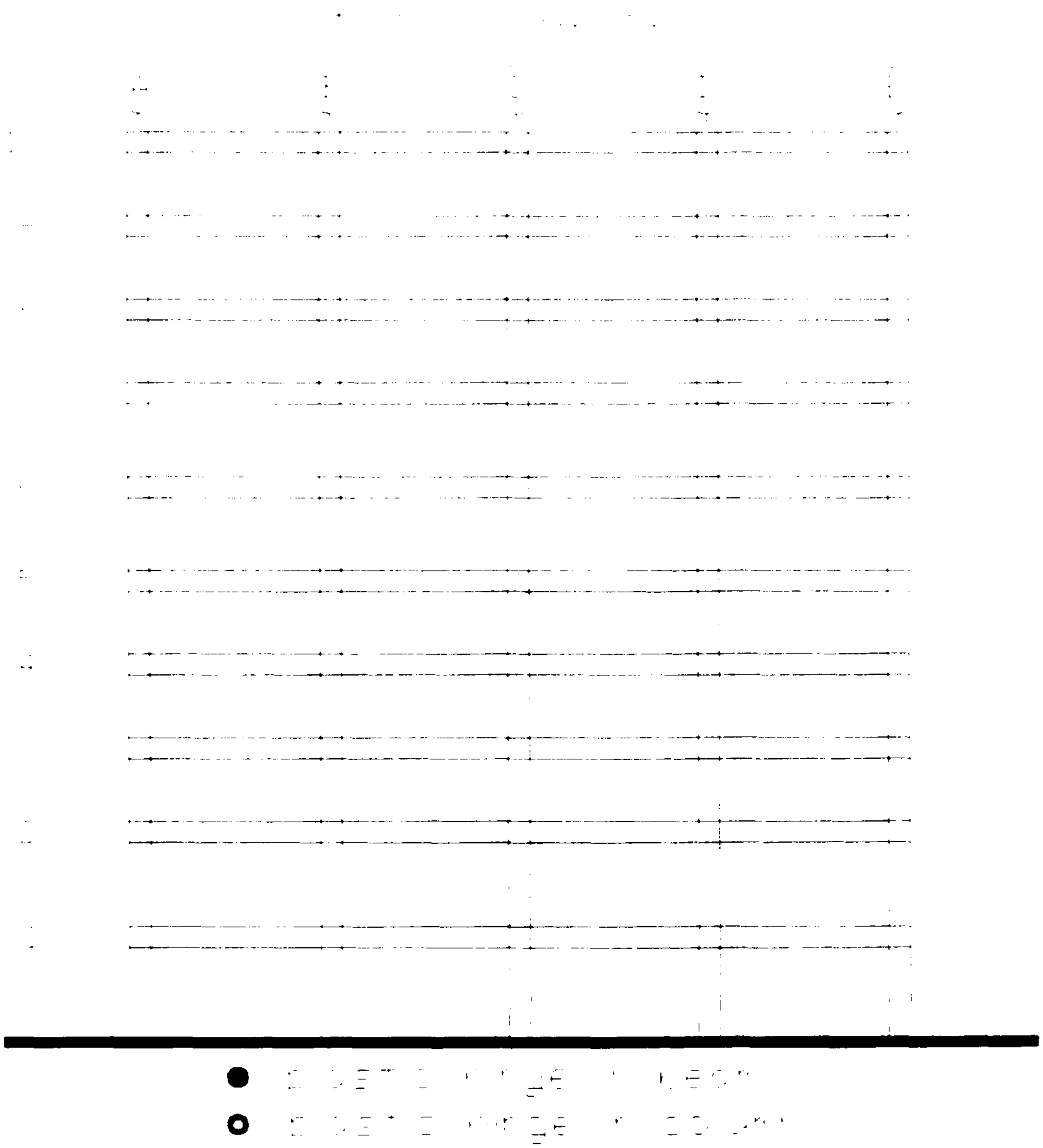

Figure 3.25. Plastic hinges in interior longitudinal frame of redesigned 10-story building after 23.34 sec. of 1.5 times the SCT, S60E, ground motion

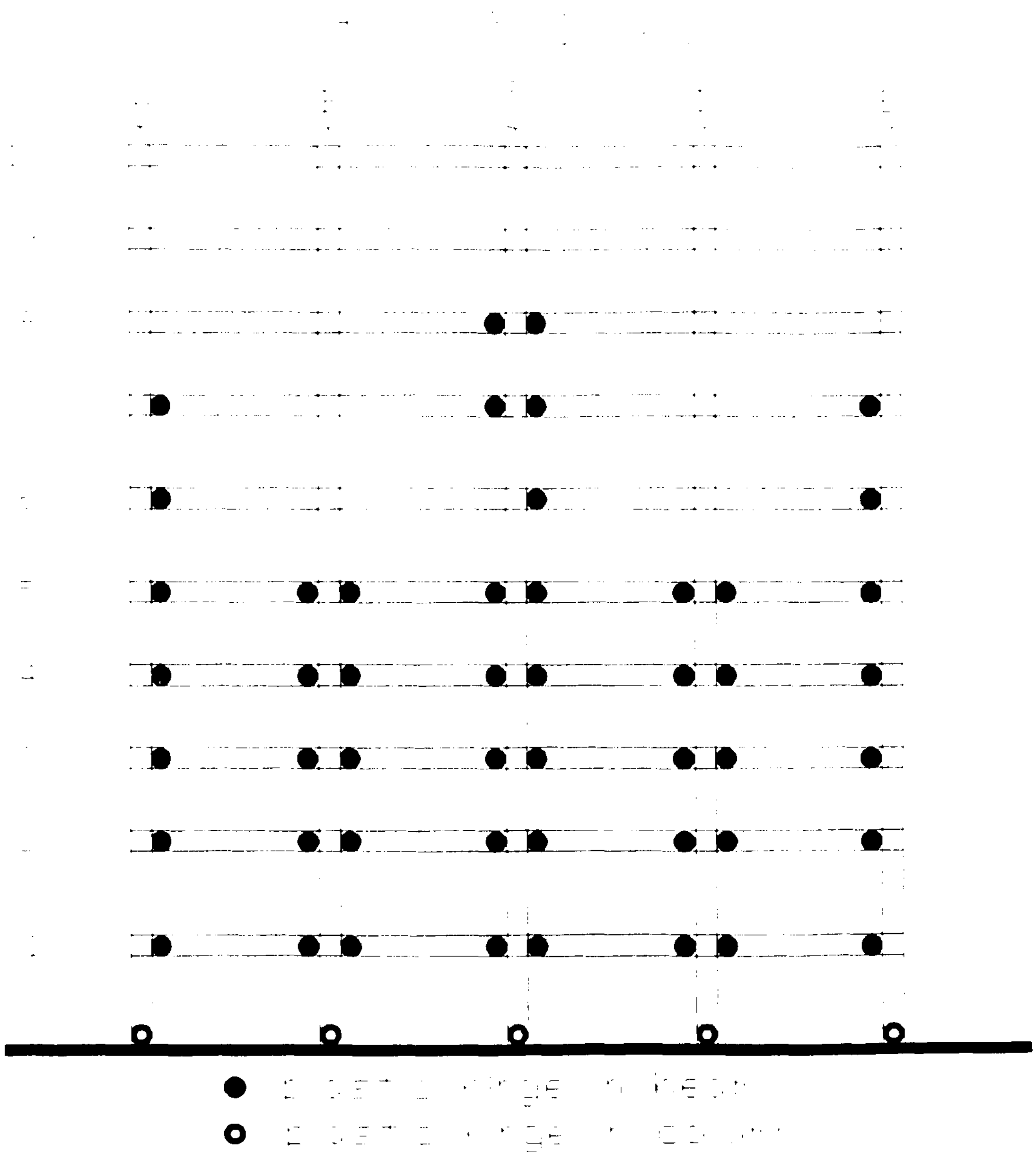

Figure 3.26. Plastic hinges in interior longitudinal frame of redesigned 10-story building after 35.01 sec. of 1.5 times the SCT, S60E, ground motion

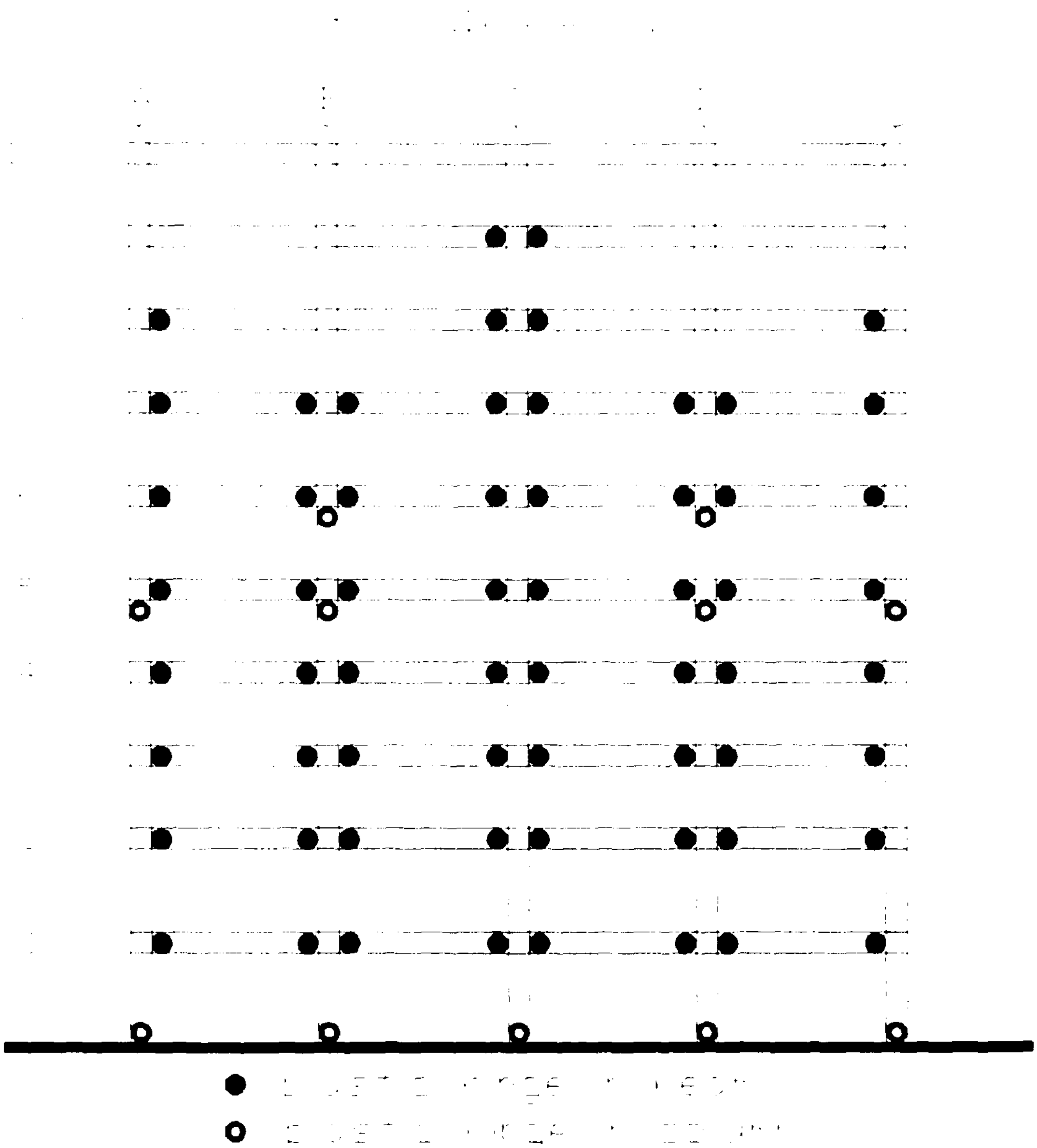

Figure 3.27. Plastic hinges in interior longitudinal frame of redesigned 10-story building after 46.68 sec. of 1.5 times the SCT, S60E, ground motion

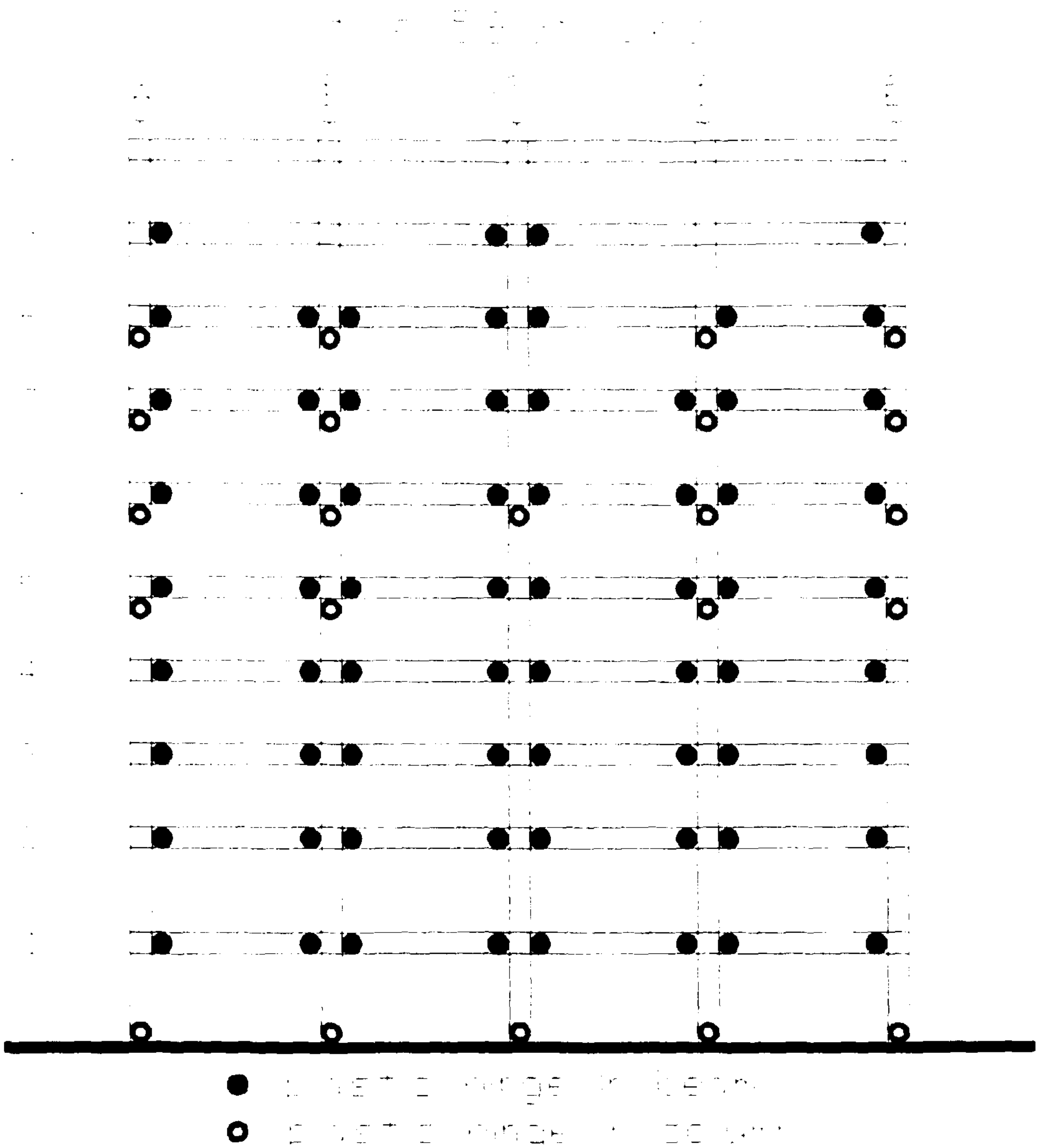

Figure 3.28. Plastic hinges in interior longitudinal frame of redesigned 10-story building after 58.35 sec. of 1.5 times the SCT, S60E, ground motion

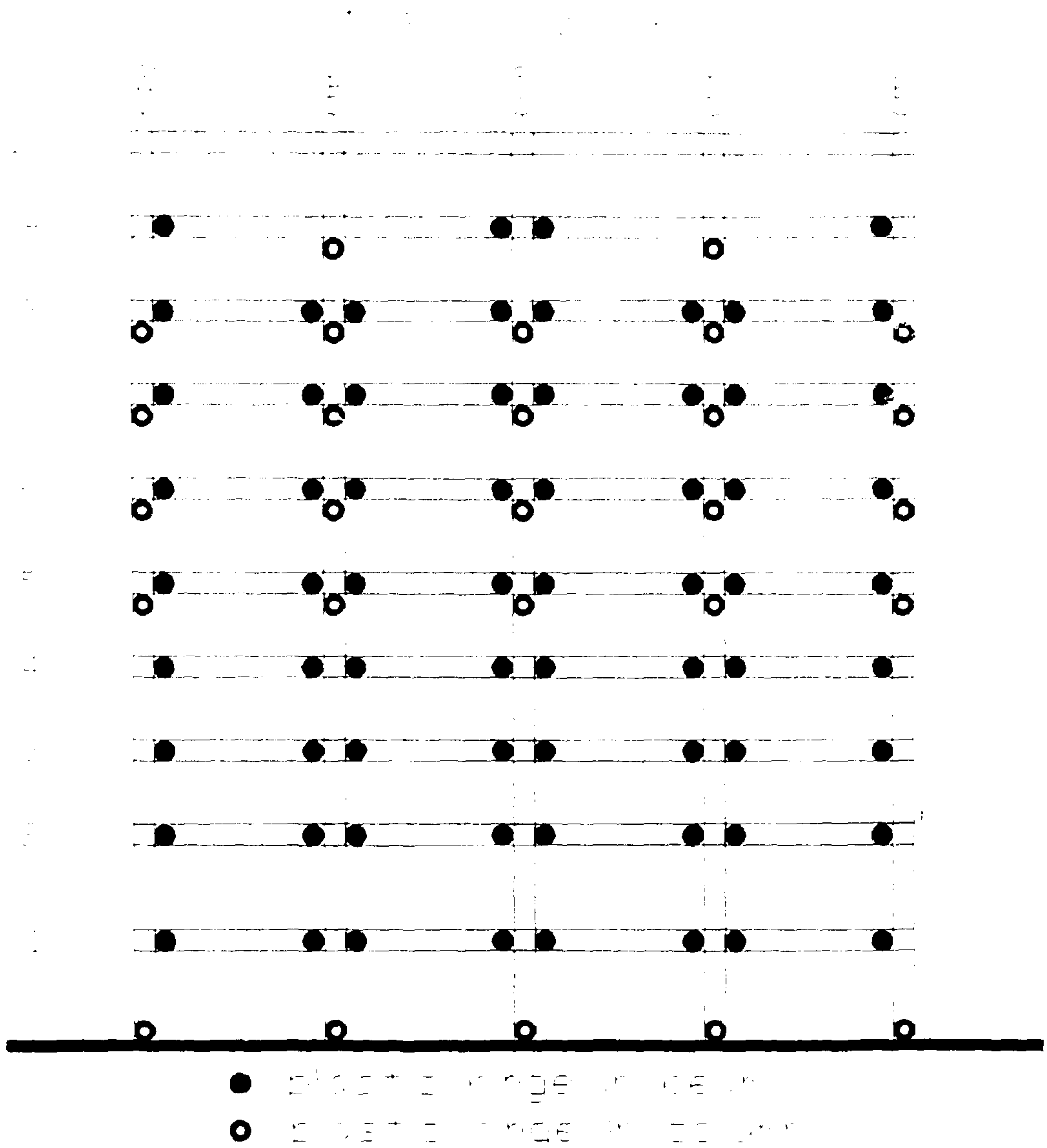

Figure 3.29. Plastic hinges in interior longitudinal frame of redesigned 10-story building after 70.02 sec. of 1.5 times the SCT, S60E, ground motion

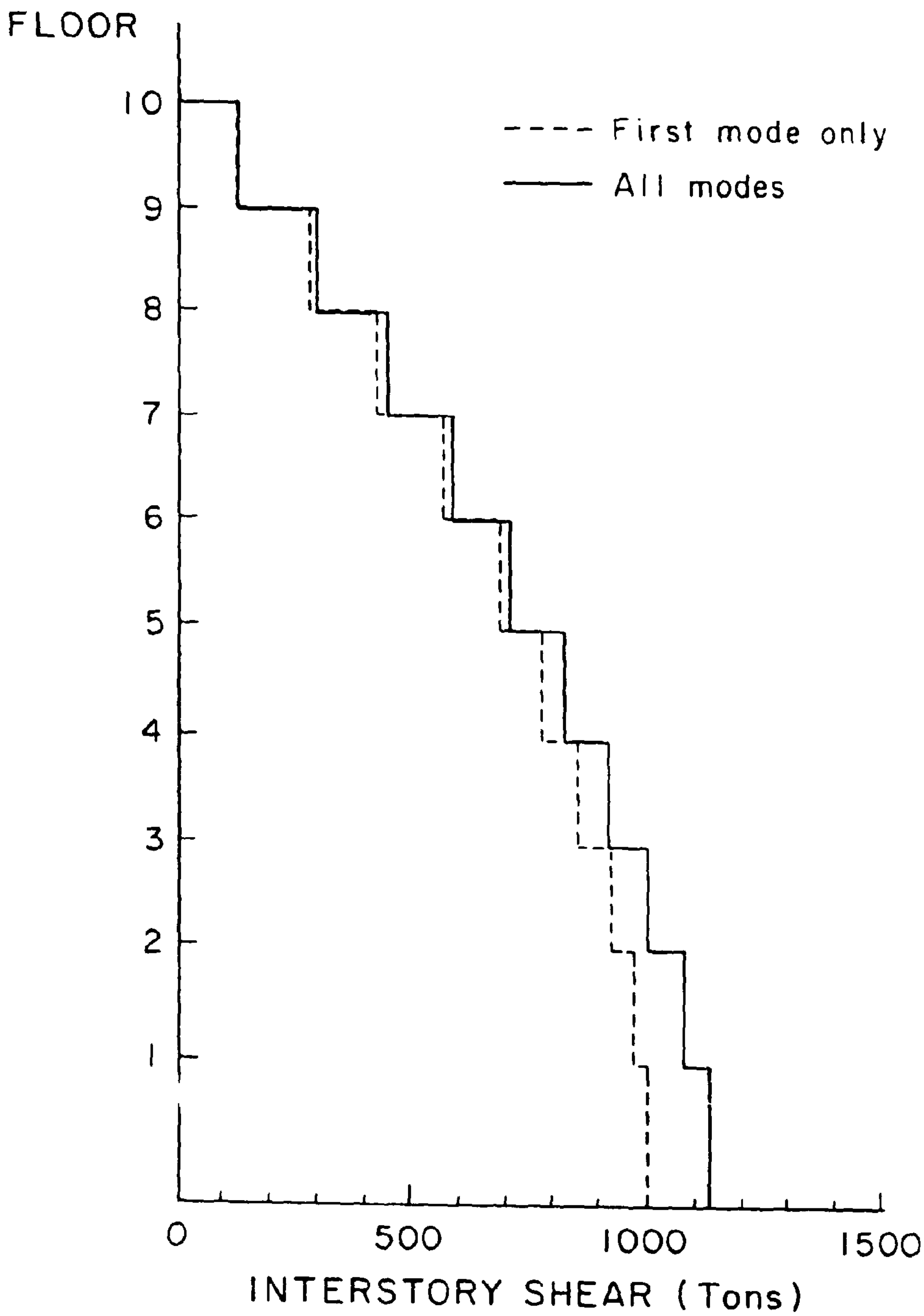

Figure 4.1. Maximum interstory shears in interior longitudinal frame of designed 10-story building when frame is assumed perfectly elastic and subjected to the SCT, S60E, ground motion.

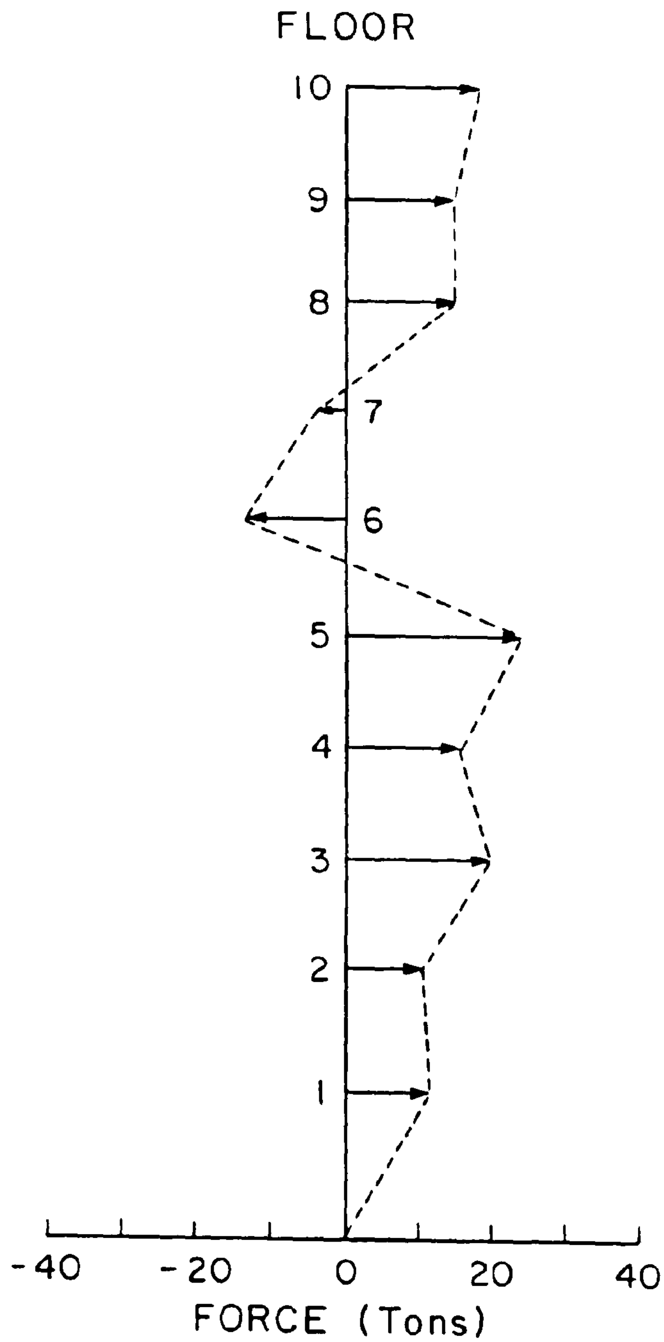

Figure 4.2. Lateral forces on interior longitudinal frame of designed 10-Story building 58.35 sec. after beginning of excitation

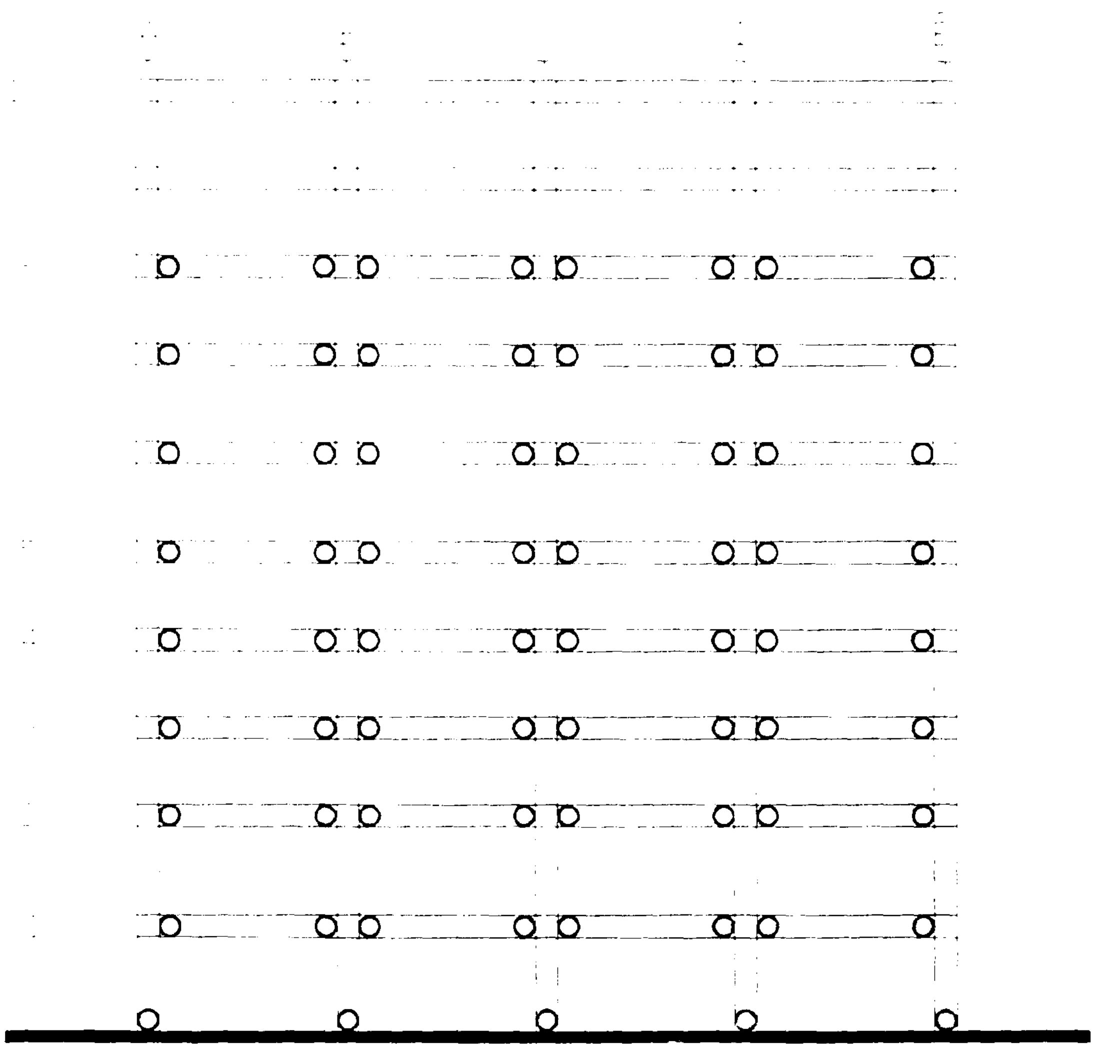

Figure 4.3. Interior longitudinal frame of designed 10-story building with regular hinges at lower ends of first-story columns and ends of beams from first to eighth floors

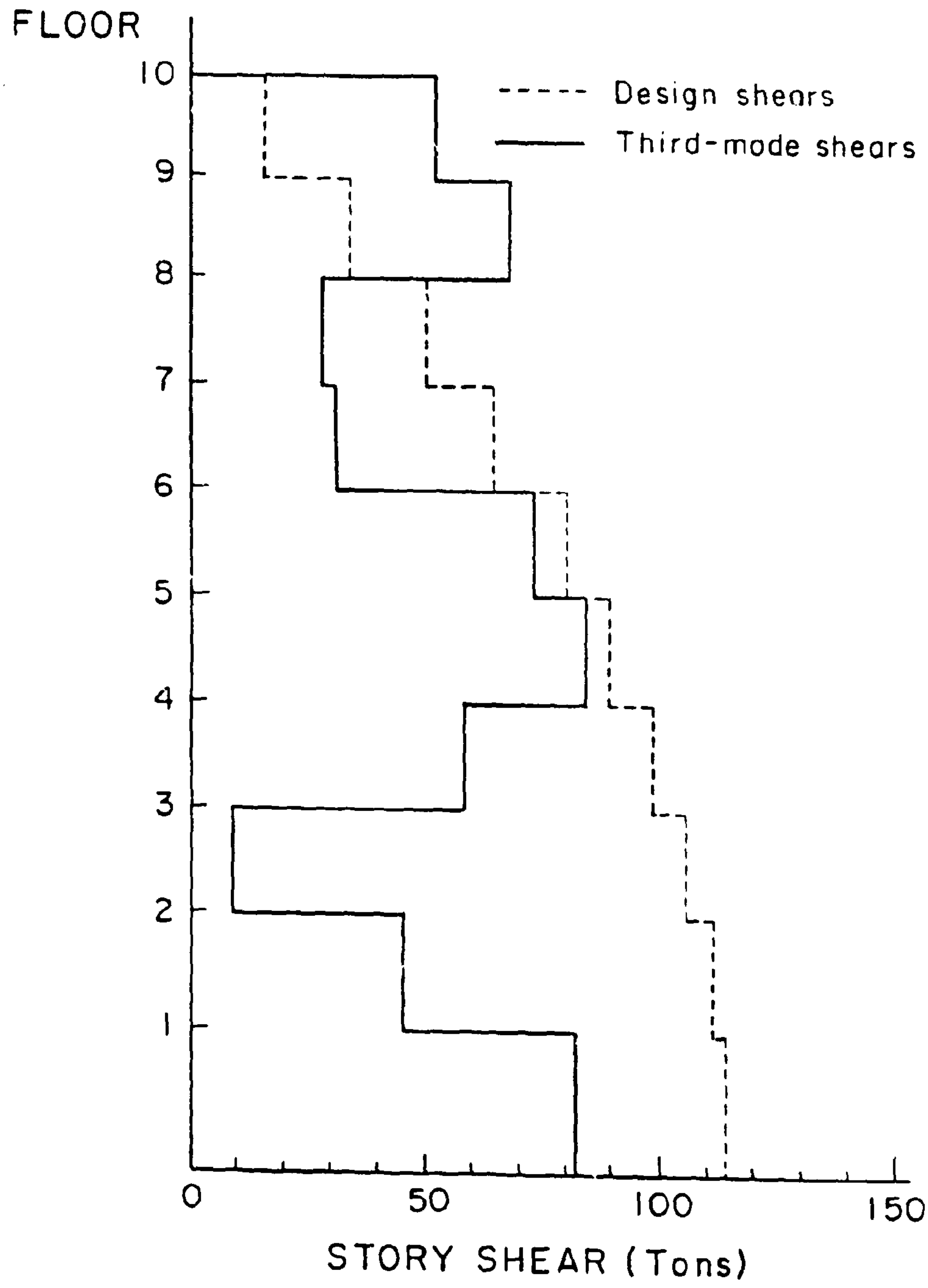

Figure 4.4. Absolute values of interstory shears in interior longitudinal frame of designed 10-story building